DEVELOPING NOVEL LEAD COMPOUNDS FOR KYNURENINE MONOOXYGENASE INHIBITION

by

EMMA CARINE IRADUKUNDA

(Under the Direction of Robert S. Phillips)

ABSTRACT

Neurodegenerative diseases such as Huntington's and Alzheimer's diseases are incurable and are among the top ten leading causes of death globally. Though their symptoms vary, they are all multifactorial and have overlaps in their etiologies. Therefore, these diseases share common therapeutic targets. Enzymes are the key factors behind biological pathways and without their activities, a lot of metabolic reactions will not take place; therefore, they comprise a large number of pharmacological targets. My dissertation focused on enzymes on the kynurenine pathway (KP) of the tryptophan pathway (TP) that are directly involved in neurodegeneration through N-methyl-D-aspartate receptor (NMDAr) regulation and free radical generation. Kynurenine (KYN) on the KP is at the key point of the KP where it acts as a substrate of three enzymes: kynurenine aminotransferase (KAT), kynurenine monooxygenase (KMO) as well as kynureninase (KYNU). When catalyzed by KAT, KYN converts to a neuroprotective metabolite kynurenic acid (KA), when catalyzed by KNYU, KYN converts into anthranilic acid which subsequently hydroxylates into a free radical generator 3-hydroxyanthranilic acid (3-HAA), and lastly, KYNU converts to another free radical generator 3-hydroxykynurenine (3-HK) through the action of KMO which later leads to 3-HAA and a neurotoxic quinolinic acid (QA). Though KYN is a substrate for the above three enzymes, it has more affinity to KMO which makes it a great target against neurodegeneration. Inhibiting KMO has not only shown to eradicate the

above neurotoxic metabolites but also shifts the KP towards neuroprotection. We have proposed several lead compounds capable of inhibiting KMO using pharmacophore modeling and structure-activity relationship. Some of these compounds not only inhibit KMO but also inhibit KYNU making them more interesting as they multitarget enzymes that are involved in the free radical generation and NMDAr agonism. In this work, we also propose a known FDA-approved NSAID agent Fenbufen to inhibit KMO in the nanomolar range, making it a viable lead compound worth drug-repurposing consideration.

INDEX WORDS: Inhibitors, Free radical generators, Kynurenine, Kynurenine Monooxygenase, Kynurenine Pathway, NMDAr, Neurodegeneration, Oxidative stress.

DEVELOPING NOVEL LEAD COMPOUNDS FOR KYNURENINE MONOOXYGENASE INHIBITION

by

EMMA CARINE IRADUKUNDA

B.S. Biochemistry, Spelman College, 2015

A Dissertation Submitted to the Graduate Faculty of The University of Georgia in Partial Fulfillment of the Requirements for the Degree

DOCTOR OF PHILOSOPHY

ATHENS, GEORGIA

2021

DEVELOPING NOVEL LEAD COMPOUNDS FOR KYNURENINE MONOOXYGENASE INHIBITION

by

EMMA CARINE IRADUKUNDA

Major Professor: Robert S. Phillips

Committee: Richard Morrison
Jeffrey Urbauer

Electronic Version Approved:

Ron Walcott
Vice Provost for Graduate Education and Dean of the Graduate School
The University of Georgia
May 2021

DEDICATION

This is for you Maman, Papa, Umutoniwase Aliane, Bizimana Amani Yvon Bruno and Irakoze Divin Garnaud, we made it!

Icyo gihe Yezu yungamo ati «Dawe, Mutegetsi w'ijuru n'isi, ngushimiye ko ibyo wabihishe abanyabwenge n'abahanga, ukabihishurira abaciye bugufi. Koko, Dawe, ni ko wabyishakiye.

Mt. 11:25-26

ACKNOWLEDGEMENTS

I would like to start by acknowledging all God's blessings and care throughout my academic journey. I thank you Most High, for every scholarship, every opportunity, every good teacher and mentor, every help, and every light-bulb moment. I surely would have never made it this far without Your unconditional love and providence.

I would like to express my deepest appreciation to you Dr. Robert Phillips for allowing me the opportunity to join your lab and learn from you when I needed it most. You are indeed among the best researchers and mentors I have ever met. I would not have made it through this program without your unwavering help, patience, and guidance. I would also like to thank my committee members (Dr. Richard Morrison and Jeffery Urbauer) for your feedback on my work and encouragements along the way.

I would like to thank you Mujuni Patrick, my high school chemistry teacher, whose inspiration led me to pursue higher education in the US. Thank you for helping me to see the hidden treasures of chemistry and to appreciate it to the atomic level. Many thanks go to you Ingabire Joselyne, for teaching me mathematics from scratch and making sure that I not only understand it, but also love it. Since I needed all As to make it to the US, I will forever be indebted to you for making sure I get that "A" in math in the National exam. I would like to thank Dr. Kimberly Jackson and Ms. Renee Shaw for mentoring me at Spelman college and for introducing me to drug discovery and eventually leading me to grad school. Many thanks to Dr. Henry Schaeffer, for believing and encouraging me throughout my graduate studies.

I am deeply indebted to my parents and siblings, thank you for believing in my ability to earn a doctorate. Every school fee, phone calls, encouragement, and advice went a long way. We surely made it. Thank you Nadege for the countless hours you spent listening to my presentations,

reviewing my work, giving me insights, encouraging me, and making sure I stay sane. Thank you, Olivier Ndicunguye, my love, for your encouragements, love, and support even from afar: it has made a lot of difference.

Last and certainly not least, I do not know what it would have been without having a Catholic center at UGA. Finally, I would like to thank all my friends, extended family members, and teachers that contributed to my success, but I did not acknowledge it explicitly. It surely takes a whole village to raise a doctor.

TABLE OF CONTENTS

Page

ACKNOWLEDGEMENTS v

LIST OF TABLES ix

LIST OF FIGURES x

LIST OF ABBREVIATIONS xii

CHAPTER

1 Introduction and Literature Review 1

Current Biological Targets for Neurodegenerative Disorders 1

Kynurenine pathway and its involvement in neurodegenerative diseases 3

Kynurenine Monooxygenase 6

Reaction Mechanism of KMO 6

KMO Structure and Species 7

KMO Inhibition 10

2 5-Nitrokynurenine 20

Abstract 21

Introduction 22

Methods 24

Results and Discussion 27

Conclusion 30

3 (*S*-(2-Aminophenyl)-L-cysteine S, S-dioxide 31

Abstract 32

Background 33
Results and Discussion 36
Conclusions 38
4 Tertiary Sulfonylureas 40
Abstract 41
Background 42
Results and Discussion 44
Conclusions 49
5 Phenyl Alkanoic Acid 50
Abstract 51
Introduction 52
Material and methods 56
Result and Discussion 60
Conclusions 65
6 Conclusions and Future Directions 67
References 70

LIST OF TABLES

Page

Table 1.1: Substrate analogs of KMO.....13

Table 1.2: Non-substrate analogs of KMO.....14

Table 4.1: Binding affinities of compounds A, B, and C on NOX vs chKMO.....46

Table 5.1: Binding affinities (K_D) of proposed phenyl alkanoic acids.....59

LIST OF FIGURES

Page

Figure 1.1: Most common biological targets for neurodegenerative diseases.....2

Figure 1.2: Kynurenine Pathway 5

Figure 1.3: Schematic of the mechanism of the KMO. 7

Figure 1.4: Sequence alignment of pfKMO, hKMO, chKMO, and scKMO.....9

Figure 1.5: A schematic overview of substrate analogs KMO inhibitors.....12

Figure 1.6: A schematic overview of non-substrate analogs KMO inhibitors. 16

Figure 2.1: Schematic overview of kynurenine pathway.....23

Figure 2.2: A structure of our proposed KMO ligand (5-NKyn).....23

Figure 2.3: HPLC analysis of 5-NKyn reaction with KMO 29

Figure 2.4: Active site of yeast KMO (PDB code: 4j36) in complex with 5-NKyn.....30

Figure 3.1: Kynurenine pathway.....34

Figure 3.2: Structure of KYN (A) and SAPCO (B).....35

Figure 3.3: (A) Fluorescence quenching in the titration 1μM KMO.FAD with SAPCO (0–27μM). (B) Change in FAD fluorescence versus free SAPCO. 36

Figure 3.4: Sequence alignment of commonly used KMO species 37

Figure 4.1: Kynurenine pathway. 43

Figure 4.2: Structures of proposed sulfonylureas for KMO inhibition.....44

Figure 4.3: Binding affinities and binding modes of compound A, B, and C. 48

Figure 5.1: Kynurenine pathway highlighting neuroactive metabolites.....53

Figure 5.2: Structures of phenyl alkanoic acids evaluated in chapter 5.....55

Figure 5.3: FDA-approved NSAID Fenbufen and PAA-1. 56

Figure 5.4: active site of scKMO in complex with PAA-1 and the binding affinity of PAA-1. ...61

Figure 5.5: active site of scKMO (PDB code: 4J34) in complex with PAA-2.....62

Figure 5.6: active site of scKMO in complex with Fenbufen and its binding affinity. 63

Figure 5.7: active site of scKMO in complex with PAA-3 its binding affinity.....64

Figure 5.8: The structure of scKMO bound to FAD and PAA-4 (A) and PAA-5 (B). 65

LIST OF ABBREVIATIONS

3-HAA	3-hydroxyanthranilic acid
3-HAO	3-hydroxyanthranilic acid oxygenase
3-HK	3-hydroxy-L-kynurenine
°	Degrees
°C	Degrees Celsius
Å	Ångström
AD	Alzheimer's disease
AP	Acute pancreatitis
CNS	Central nervous system
CSF	cerebrospinal fluid
ch	*Cytophaga hutchinsonii*
Da	Daltons
DMSO	Dimethyl sulfoxide
DNA	Deoxyribonucleic acid
DTT	Dithiothreitol
E. coli	*Escherichia coli*
EDTA	Ethylenediaminetetraacetic acid
FAD	Flavin adenine dinucleotide
g	Gravity
g (ng/µg/mg/kg)	Grams (nano/micro/milli/kilo)
h	Human
HD	Huntington's disease

HEPES	4-(2-hydroxyethyl)-1-piperazineethanesulfonic acid
HPLC	High pressure liquid chromatography
IC50	Half maximal inhibitory concentration
KA	Kynurenic acid
KAT	Kynurenine aminotransferase
kcat	Turnover number
Ki	Dissociation constant of inhibitor
KM	Michaelis-Menten constant
KMO	Kynurenine 3-monooxygenase
KP	Kynurenine pathway
KYN	Kynurenine
KYNU	Kynureninase
L(nL/µL/mL)	Liter (Nano/micro/milli)
LB	Luria Bertani
L-kyn	L-kynurenine
L-Trp	L-tryptophan
M (nM/µM/mM)	Molar (nano/micro/milli)
m (nm/mm)	Meter (nano/milli)
min	Minutes
MW	Molecular weight
NAD/NAD+	Nicotinamide adenine dinucleotide
NADPH/NADP+	Nicotinamide adenine dinucleotide phosphate
NMDAr	N-methyl-D-aspartate receptor
NOX	Nicotinamide adenine dinucleotide phosphate oxidase

OD600	Optical density at 600 nm
OS	Oxidative stress
PAGE	Polyacrylamide gel electrophoresis
PCR	Polymerase chain reaction
PDB	Protein data bank
PEG x	Poly-ethylene glycol, the average molecular weight of x
Pf	*Pseudomonas fluorescens*
PHBH	Para-hydroxybenzoate hydroxylase
PLP	Pyridoxal 5'-phosphate
p-OHB	Para-hydroxybenzoate
QA	Quinolinic acid
ROS	Reactive oxygen species
rpm	Revolutions per minute
s	Seconds
Sc	*Saccharomyces cerevisiae*
SDS	Sodium dodecyl sulfate
UV	Ultraviolet
Vis	Visible
w/v	Weight/Volume
w/w	Weight/weight

CHAPTER 1

INTRODUCTION AND LITERATURE REVIEW

Current biological targets for neurodegenerative disorders

According to the Harvard NeuroDiscovery center, about 5 million Americans have Alzheimer's disease and the same study estimates that if no action is taken, 30 years from now, more than 12 million Americans will suffer from neurodegenerative diseases [2]. However, finding, optimizing, and validating biological targets for any indication or disease, is crucial in ensuring success for any drug discovery adventure[3]. The two common ways to identify biological targets early in the drug discovery are forward chemical genetics (phenotype-based approaches) [4]and reverse genetics (target-based approaches) [5]. The forward chemical genetics consists of assessing the phenotype change in a biological system by perturbing it with various small molecules followed by studies of mechanisms of actions to determine the protein/gene responsible for the change in phenotype. On the other hand, reverse genetics consists of identifying and validating a protein/gene in a disease responsible for a certain phenotype before determining the mechanism of action. My work utilizes the latter in identifying lead compounds suitable for neurodegenerative disease treatment.

Though several diseases/disorders such as sickle cell anemia and cystic fibrosis only involve one gene, some other diseases have much more complex mechanisms and are multifactorial. Therefore, their therapeutic approaches involve targeting more than one gene/biological entity[6-8].

Given the multifactorial nature of complex diseases such as neurodegenerative diseases, multi-targeting or combination therapy seems to be inevitable[9].

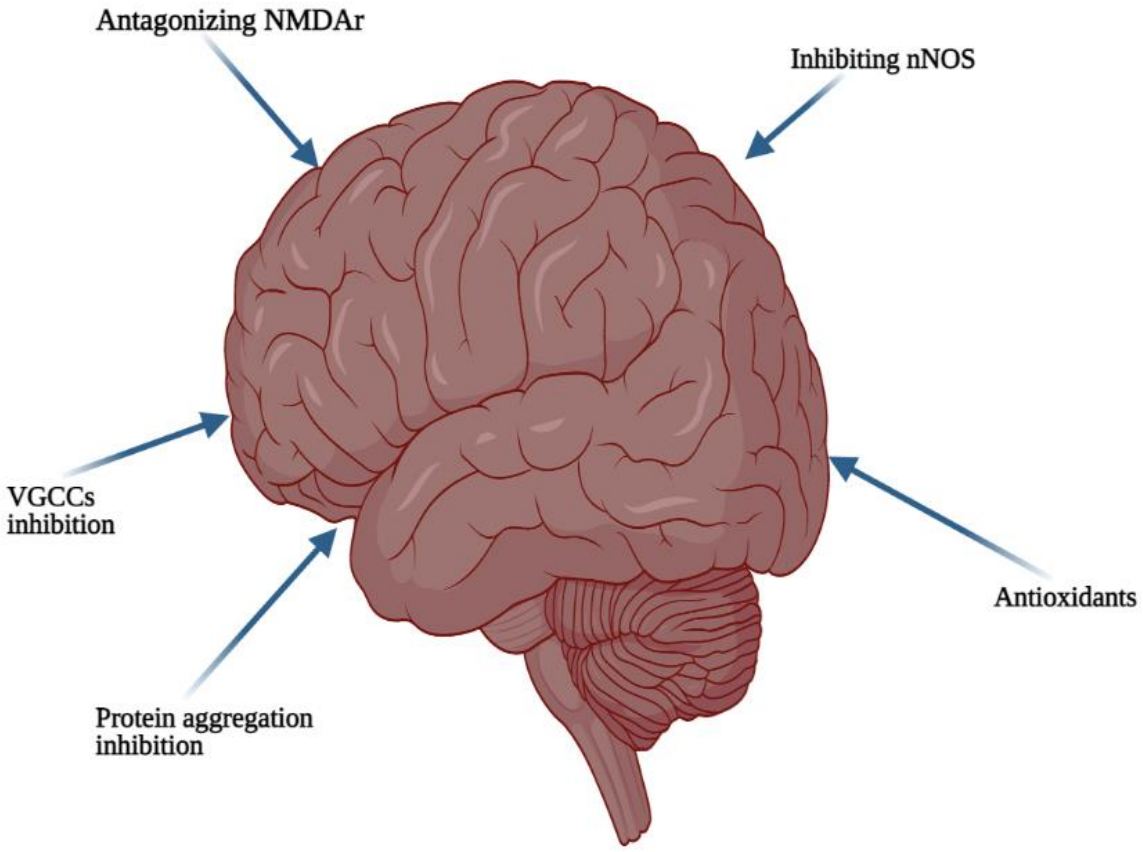

Figure 1.1 Most common biological targets for neurodegenerative diseases.

The five most common biological targets (Figure 1.1) for neurodegenerative diseases are NMDAr[10, 11], voltage-gated calcium channels (VGCCs) [12, 13], neuronal nitric oxide synthase (n-NOS) [14], oxidative stress (OS) from ROS [15, 16]as well as protein aggregation [17-19].

This work focuses on enzymes that are involved in NMDAr regulation as well as OS.

NMDAr is an ionotropic ligand-gated and voltage-dependent receptor that responds to glutamate and NMDA. Like VGCCs, it allows the flow of calcium ions (Ca^{2+}) through the postsynaptic cells. In the normal organism, the release of Ca^{2+} ions is essential in the synaptic transmission [20]. However, the overstimulation of VGCC and NMDAr leads to the influx of the Ca^{2+} ions causing neuron damage[21]. Additionally, the increase of intracellular Ca^{2+} ions activate the nNOS leading to the accumulation of reactive oxidative species (ROS) and hence to oxidative stress (OS). Oxidative stress is one of the conditions behind the development of many diseases such as cardiovascular diseases and neurodegenerative disorders [22]. The brain is among the top single organs that utilize a lot of oxygen[23]; however, this utilization is high in comparison to the concentration of antioxidants, therefore, the central nervous system (CNS) is vulnerable to OS[24]. The presence of ROS such as hydrogen peroxide(H_2O_2), free radicals, and hydroxyl radicals leads to OS. The accumulation of ROS in the CNS is responsible for the initiation and progression of neurodegeneration by causing neuron damage [25]. Therefore, antagonizing the NMDAr and/or inhibiting enzymes involved in free radical generation is a current and promising therapeutic target for neurodegenerative disease.

Kynurenine pathway and its involvement in neurodegenerative diseases

The kynurenine pathway (KP) is the primary route for tryptophan catabolism. About 90% of ingested L-tryptophan (L-Trp) enters the kynurenine pathway and only 10% goes into the serotonin and melatonin pathway as well as protein synthesis [26, 27]. Depending on which organ the KP takes place, one of the following dioxygenases: tryptophan2, 3-dioxygenase (TDO), indoleamine 2, 3-dioxygenase 1 (IDO1), and indoleamine 2, 3-dioxygenase 2 (IDO2) catalyzes the oxidative cleavage of L-Trp to N-formyl-kynurenine (NFK). TDO is expressed

predominantly in the liver, whereas IDO1 and IDO2 are expressed in various other tissues [28]. Subsequently, kynurenine formidase rapidly converts NFK to L-kynurenine (L-kyn). As shown in Figure 1.2, L-kyn is at the branch point of KP where one of the three enzymes catalyzes L-kyn to make biologically active metabolites. For instance, if L-kyn follows the kynurenine monooxygenase (KMO) path, it leads to the production of 3-hydroxykynurenine (3-HK) which further metabolizes to 3-hydroxyanthranilic acid (3-HAA) and quinolinic acid (QA); both 3-HK and 3-HAA are free radical generators and hence neurotoxic. QA is an NMDAr agonist and a neurotoxin that leads to both human neuronal death and dysfunction. Recent studies have revealed lipid peroxidation to be a major route/mechanism of QA neurotoxicity [29-32]. On the other hand, if L-kyn follows the kynurenine aminotransferase (KAT) path, it produces a neuroprotective metabolite: kynurenic acid (KA) [33]. Unlike QA, KA is an NMDAr antagonist, thus neuroprotective. It is known to antagonize some of the effects of QA toxicity [34]. However, the amounts of QA in cerebrospinal fluid (CSF), brain, and systemic circulation are much higher than that of KA (about 15 fold), which makes KA neuroprotection insufficient [35].

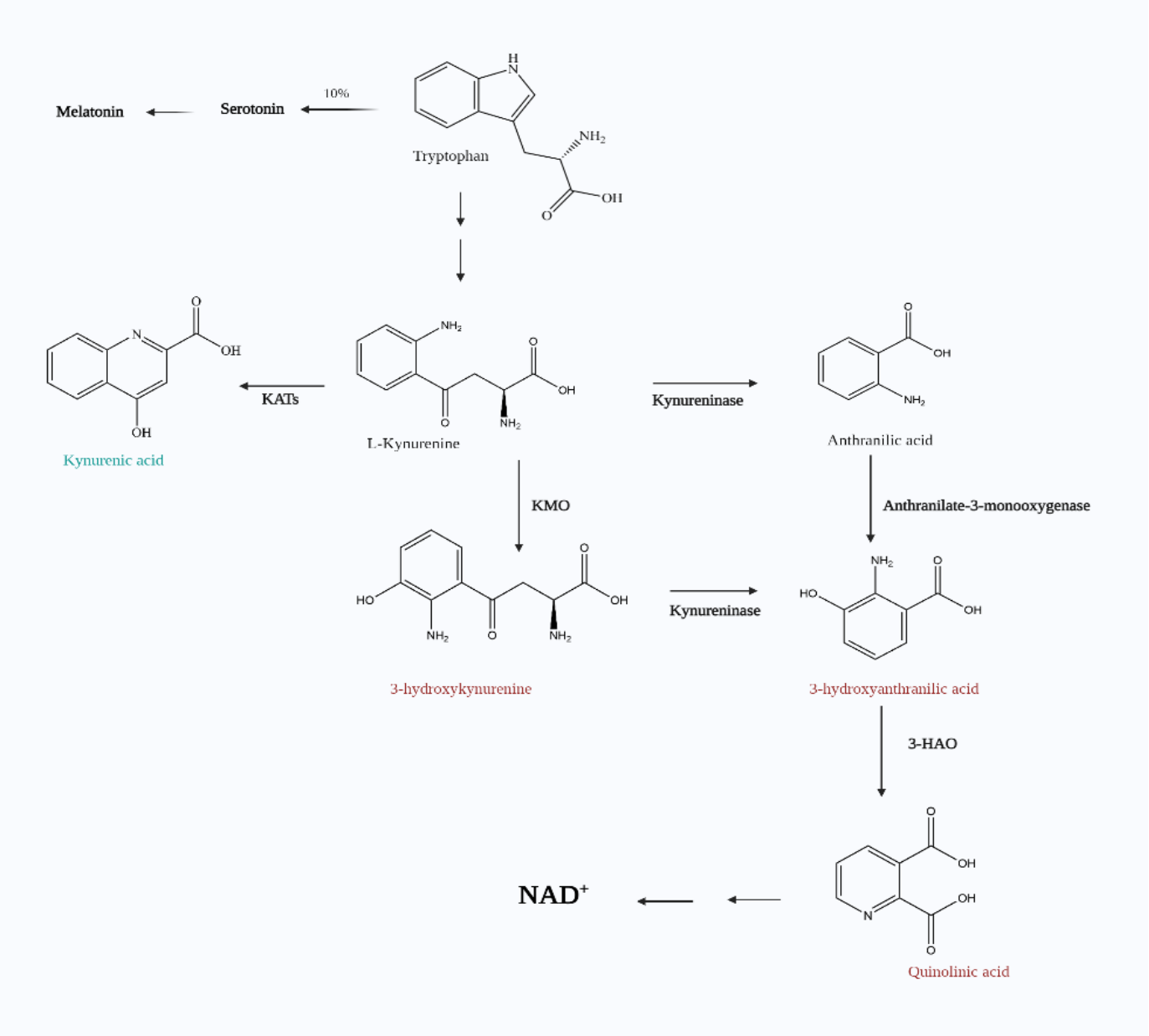

Figure 1.2. Kynurenine Pathway

Interest in the KP was long centered on its importance as a source of nicotinamide (NAD^+), but further studies have revealed its evident involvement in various diseases such as Acute pancreatitis [36], major depression disorder [37], schizophrenia and bipolar disorder[38], Alzheimer's [39], Huntington's [40], and Parkinson's [41] diseases. Thus, enzymes on KP such as dioxygenases, KAT,

KMO, kynureninase (KYNU) as well as KAT have emerged as a therapeutic target for the above diseases.

There is only 1 μM of KA available in the brain, however, studies had shown that about 10-1000 μM of KA is needed to block the NMDA receptor [42]. Several strategies to regulate NMDAr homeostasis were proposed and all of them seek to increase the KA levels in the brain by seizing both QA, 3-HAA, and 3-HK. Since KA does not cross the brain-blood barrier (BBB) appreciably, KMO inhibition seems to be the ideal pharmacological strategy since it does not only does it eradicate the above-mentioned detrimental metabolites, but also increases the L-kyn levels in the brain to further synthesize more KA [43].

Kynurenine monooxygenase

KMO is an NADPH-dependent flavoenzyme located in the outer mitochondria. It is primarily expressed in the liver and kidney and less in the brain in microglia and infiltrating macrophages. However, KMO expression is increased in inflamed cells such as in events of neurodegeneration. [44, 45]. This section will discuss KMO's reaction mechanism and its structure information as well as its important role as a drug target for neurodegenerative diseases.

Reaction mechanism

KMO is an NADPH-dependent flavoenzyme [46]. Like other monooxygenases, it catalyzes the incorporation of the hydroxyl group into the substrate using molecular oxygen and leaves water as a byproduct. The catalytic mechanism in Figure 1.3. has three major parts: substrate binding to the KMO.FAD complex, the reductive half-reaction, where NAPDH reduces FAD, and lastly, the oxidative half-reaction where the oxygen molecule binds to hydroxylate the substrate.

Figure 1.3. Schematic of mechanism of the KMO. The mechanism is divided into three main parts. Substrate binding to KMO.FAD complex (blue), reductive half-reaction (brown), oxidative half-reaction (black). The mechanism was first proposed by Moran. et. al and image adapted from Hutchinson, Jonathan P., et al.

Structure and species

KMO is expressed in nearly a thousand species. The human enzyme (hKMO) is a membrane-associated protein consisting of 486 amino acids with the hydrophobic C-termini attached to the outer membrane of mitochondria [47]. However, the purification of membrane-associated proteins like hKMO requires detergents to make them soluble [48, 49]. The use of detergent is rather

detrimental to the crystallography and as a result, the purification and crystallization of full-length hKMO have been unsuccessful. Although the systematic truncation of the C-terminal tail resulted in a normal expression of the enzyme, the enzymatic activity was completely abolished indicating a pivotal role of the C-terminal in hKMO function[1, 50]. Therefore, kinetic studies of KMO were performed using the enzyme from other species notably *Pseudomonas fluorescens* (pfKMO) and yeast/*Saccharomyces cerevisiae* (scKMO). The first KMO structure to be solved was from scKMO, it has 38% sequence identity and 51% similarity to hKMO [1]. It only consisted of 396 amino acids from N-terminal with an entirely missing α-C-terminal domain, the role of the C-terminus in the enzymatic activity of scKMO is still not known. However, unlike in hKMO, the truncation of the C-terminus did not affect the enzymatic activity. On the other hand, the prokaryotic KMO is not membrane-associated, making the C-terminal less hydrophobic, thus the structure of full-length pfKMO was also solved [51]with 36% sequence (Figure 1.4) similarity with human and high structure similarities to scKMO despite the missing C-terminal from yeast KMO. It is also important to note that all the residues involved in FAD and substrate binding are all conserved across the above species. Despite that the active residues are highly conserved across species (Figure 1.4), research has shown that some ligands adopt different binding modes across species, resulting in NADPH uncoupling as is described in the next section. In this study, we proposed *Cytophaga hutchinsonii* (chKMO) as another species with high similarities in the active site as the yeast KMO. chKMO was first proposed and isolated by Colabroy et. Al. [52]; and ever since, our lab has performed kinetic studies using this species with various ligands as substrates, non-substrate effectors, and inhibitors of KMO. Additionally, this study provides an improved purification procedure of chKMO. We hope that the results from this species, could

very well translate to the human species, and therefore, we hope to provide a better surrogate for hKMO.

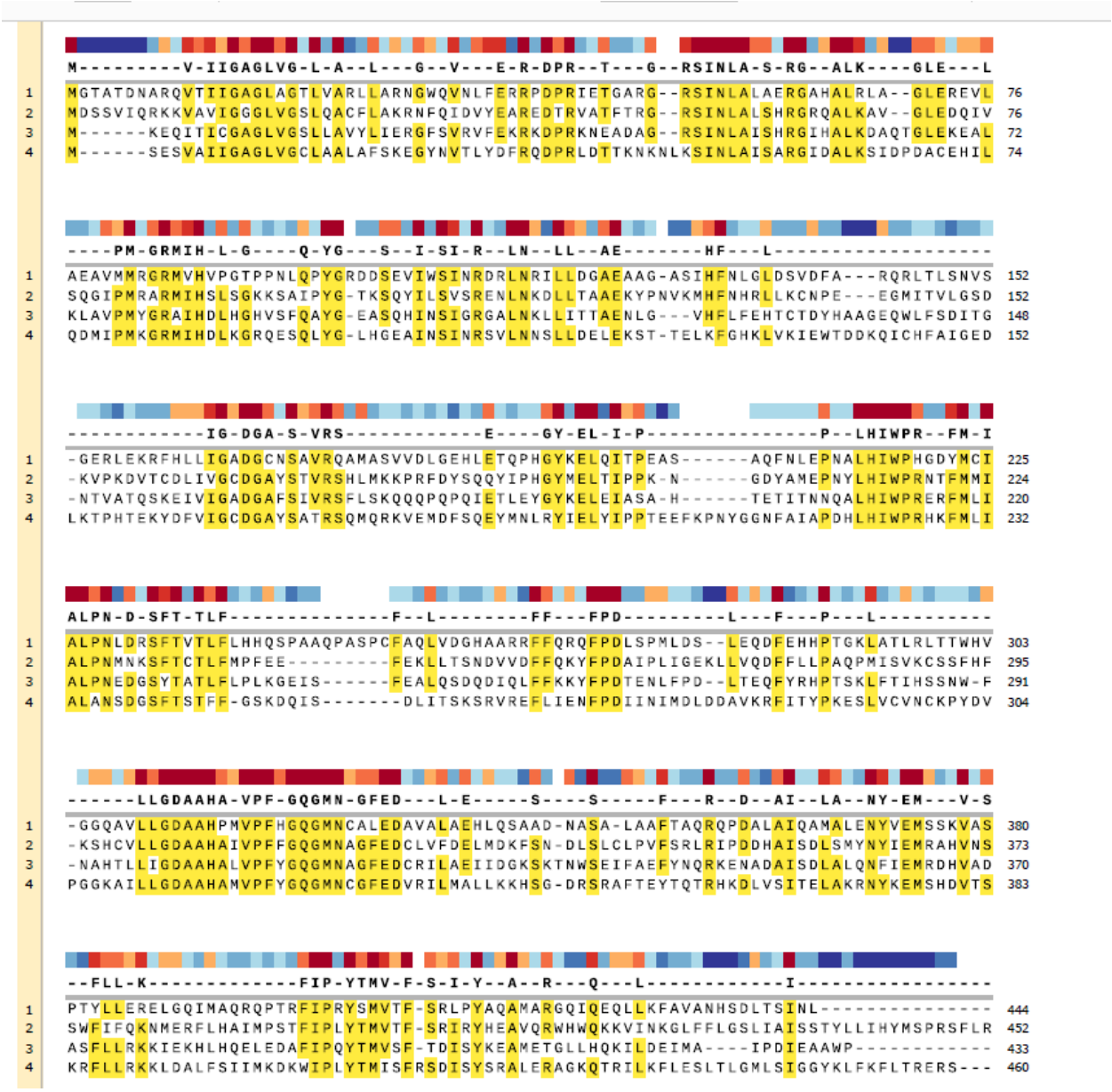

Figure 1.4. Sequence alignment of pfKMO, hKMO, chKMO, and scKMO. Alignment was generated using NCBI Blast [53]. Conserved residues across these species are marked with yellow highlighting.

Kynurenine monooxygenase inhibition

Kynurenine analogs

In the last two decades, KMO inhibition has had a lot of attention as a viable target for neurodegenerative disease treatment. However, the crystal structure of KMO was still unknown and therefore, the discoveries only relied upon mimicking the structure of the known KMO substrate L-kyn (Figure 1.5). There are many advantages of substrate analogs as potential inhibitors because they can readily bind like the physiological substrate only without producing the undesired product. The removal of an amino group from the aromatic ring of L-kyn resulted in β-Benzoyl-L-alanine (BA) (Figure 1.5, **2**) with an inhibitory potency of 7.4 μM [54]. Further manipulation of this compound by addition of a nitro group at the meta position of the ring resulted in a much more potent inhibitor (m-nitrobenzyl) alanine (m-NBA) (Figure 1.5, **3**) (IC_{50}= 0.9 μM) [43]. The in vivo studies later demonstrated that m-NBA regulates NMDA receptor agonism and antagonism homeostasis in both the brain and blood of rats. When about 400 mg/kg was administered in rats, there was an increased level of both L-kyn and KA to up 10 times and 5 times in the brain and blood, respectively.

Further modification of **3** resulted in a more potent (*R*, *S*)-3, 4-dichlorobenzoylalanine (FCE 28833A) (Figure 1.5, **4**). The addition of chlorine to the 3rd and 4th position on the benzene ring increased the inhibition potency to 4.5-fold (IC_{50} = 0.2 μM), this indicated that blocking the hydroxylation site on the ring could increase the inhibition potency of kynurenine analogs. KMO inhibition with **4** also showed an increase in kynurenine and kynurenic acid levels by 14-fold and 34-fold respectively in brain tissue[55], highlighting a shift in the KP pathway toward neuroprotection in the presence of a KMO inhibitor. Though the carboxyl group is obligatory for KMO inhibition[1], the amino group is not. Therefore, removal of the amino group and addition of

a cyclopropyl linker to the benzolyalanine portion of FCE 2883 resulted in UPF-648 with an inhibitory potency in the lower nanomolar range (IC_{50} =20 nM). Treatment of 100 μM UPF-648 has shown to shift the KP to the synthesis of KA in both the brain and plasma of fruit flies. This compound was later used in the discovery of the first-ever KMO crystal structure to be solved[1] marking the beginning of structure-based KMO ligand design. Using the co-crystallized structure of scKMO with **7**, it was shown that the carboxylate group is indeed essential in inhibition where it interacts with Arg 83 and Tyr97, two of the conserved residues in both KMO species. The aromatic moiety lay in the conserved hydrophobic pocket on the *re*-side of the FAD cofactor. Using that structural information, a structure-based pharmacophore was proposed using both scKMO as well as compound **7**[56] and predicted several inhibitors, with 3,4-dichlorohippuric acid (Figure 1.5, **6**) being the best in that library. Substituting the L-kyn at the 3rd position has shown to result in good inhibition. This is because the 3rd position is the hydroxylation site of L-kyn in the presence of KMO, making kynurenine analogs substituted at the 3rd position competitive inhibitors as shown by Phillips et.al[56]. In their study, they proposed several halogenated kynurenine analogs, and 3,5-dibromokynurenine (Figure 1.5, **5**) was the best inhibitor in their library with K_i in the low micromolar range (Table 1.1).

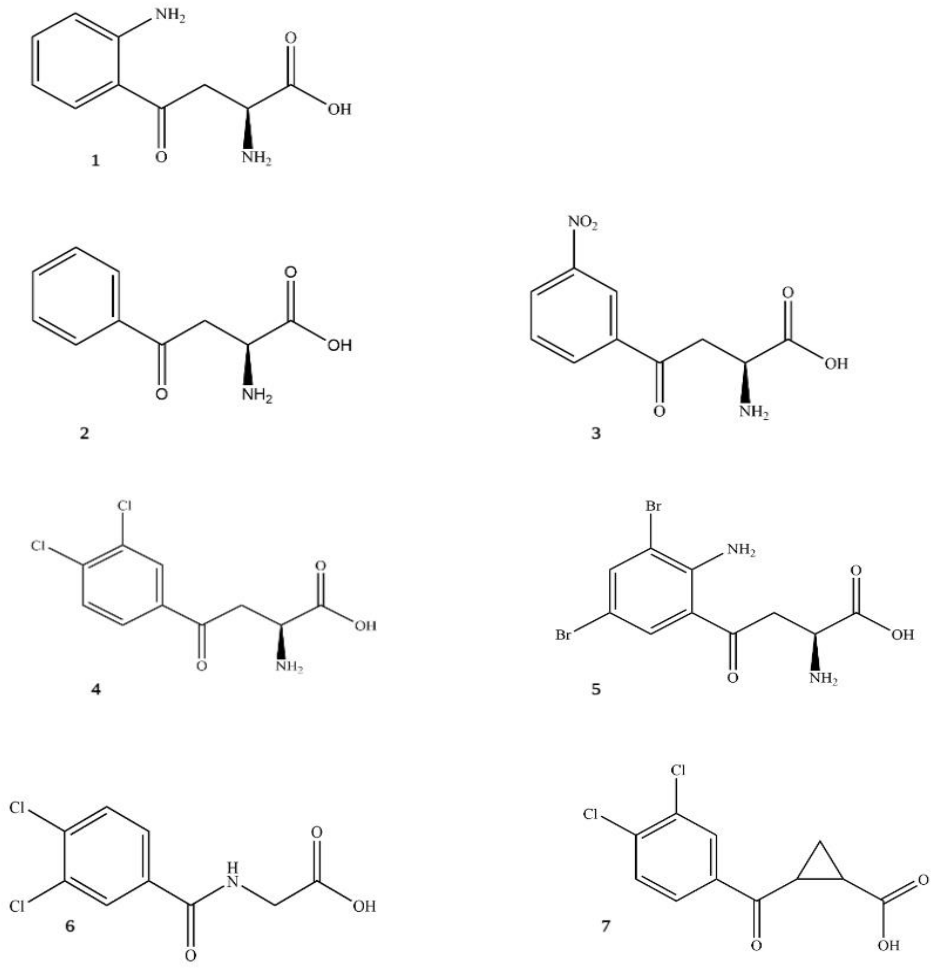

Figure 1.5. A schematic overview of substrate analogs KMO inhibitors.

Compound	Name	Binding affinity (IC_{50}) or K_d (μM)
1	Kynuurenine	17.4
2	β-Benzoyl-L-alanine	7.6
3	*m*-NBA	0.90
4	FCE28833A	0.20
5	3,5-Dibromo-L-kynurenine	1.2
6	3,4-Dichlorohippuric acid	34
7	UPF-648	0.020

Table 1.1. Substrate analogs of KMO.

Non-substrate analogs KMO inhibitors

There are several KMO inhibitor lead compounds that are not structurally similar to L-kyn. Sulfonamides were the first non-substrate analog to be examined for KMO inhibition, they provided a much better inhibitor potency compared to the previously proposed scaffolds. Ro-61-8048 (Figure 1.6, **1A)** was the best in this group with inhibition in the nanomolar range (IC_{50} = 37 nM). Though this compound does not cross the blood-brain barrier, research has shown that it raises both L-kyn and KA levels in the brain through peripheral KMO inhibition [57]. However, **1A** is not metabolically stable and therefore, an orally bioavailable slow-release prodrug (JM6, Figure 1.6, **2A)** was synthesized and tested on a transgenic mouse model with Alzheimer's diseases. The results show that it inhibited KMO in blood, and though it could not cross the blood-brain barrier either, it was able to ameliorate symptoms of neurodegeneration such as synaptic loss and spatial memory loss and reduced the extracellular glutamate in the brain[58]. This finding supports the development of carboxylic acid-containing compounds that do not meet the

BBB crossing criterion. Like **2A**, another compound isolated from *Ianthella quadrangulates*, Iannthellamide A (Figure 1.6, **3A**), had been shown to selectively inhibit KMO resulting in a significant increase in the KA levels in the rat brain.

Compound	**Name**	**Binding affinityIC50 or K_d (µM)**
1	Ro-61-8048	0.037
2	JM6	
3	PNU-168754	0.040
4	CHDI-340246	0.0005
5	GSK 366	0.0007
6	5-(3-nitrobenzyl)-1Htetrazole	6.3
7	Diclofenac	13.6

Table 1.2. Non-substrate analogs of KMO

A series of 3-oxo-propionitrile[59] was patented in the late ’90s as inhibitors of KMO, with 4A being the lead compound from the scaffold. This compound had inhibitory potency in the lower nanomolar range.

Aryl pyrimidinecarboxylic acids such as **5A** (Figure 1.6) were developed. N3 is thought to mimic the L-kyn carbonyl oxygen whereas the N1 mimics the amine group which is very essential for the inhibition. **5A** is highly selective to KMO over other enzymes on the KP and they have shown their potency both in vivo and in vitro. When 10mg/kg of **5A** was administered orally in rats, an increase in the L-kyn and KYNA and a decrease of both QA and 3HK in the brain was observed[60].

Benzisoxazoles are among the most potent and well-studied KMO inhibitors. They were examined for inhibitory potency against KMO targeting acute pancreatitis and multiple organ dysfunction syndromes. They are similar in structure with the L-kyn and have inhibitory potency in the nanomolar range. GSK 366 (Figure 1.6, **6A)** is by far the most potent among this series of the compound, with inhibitory potency in the subnanomolar range (Table 1.2). This compound binds to the active site and with a concomitant tilting of the flavin by the methylpyridazine ring that is attached to the benzisoxazole ring, which is believed to promote the potency and the residence time of the inhibition[51]. Though their potency in preventing neurodegeneration is yet to be assessed, notably the ability to cross the blood-brain barrier, they still provide exciting insights and serve as great lead compounds for future drug design and discovery for neurodegenerative disorders. A series of tetrazoles was proposed as another set of inhibitors using high throughput screening with RapidFire mass spectroscopy [61]. **7A** was a lead compound from the series with inhibitory potency in the low micromolar range (Table 1.2).

Most recently, another group proposed a molecular similarity and drug repurposing approach. Known drugs were computationally predicted and tested for KMO inhibitory capacities. Through this ligand-based approach, diclofenac (Figure 1.6, **8A**), a known anti-inflammatory drug, has been identified as a KMO inhibitor (IC_{50} = 13.6 μM). This study set a stage for future studies using molecular similarities studies as well as drug repurposing [62]. `

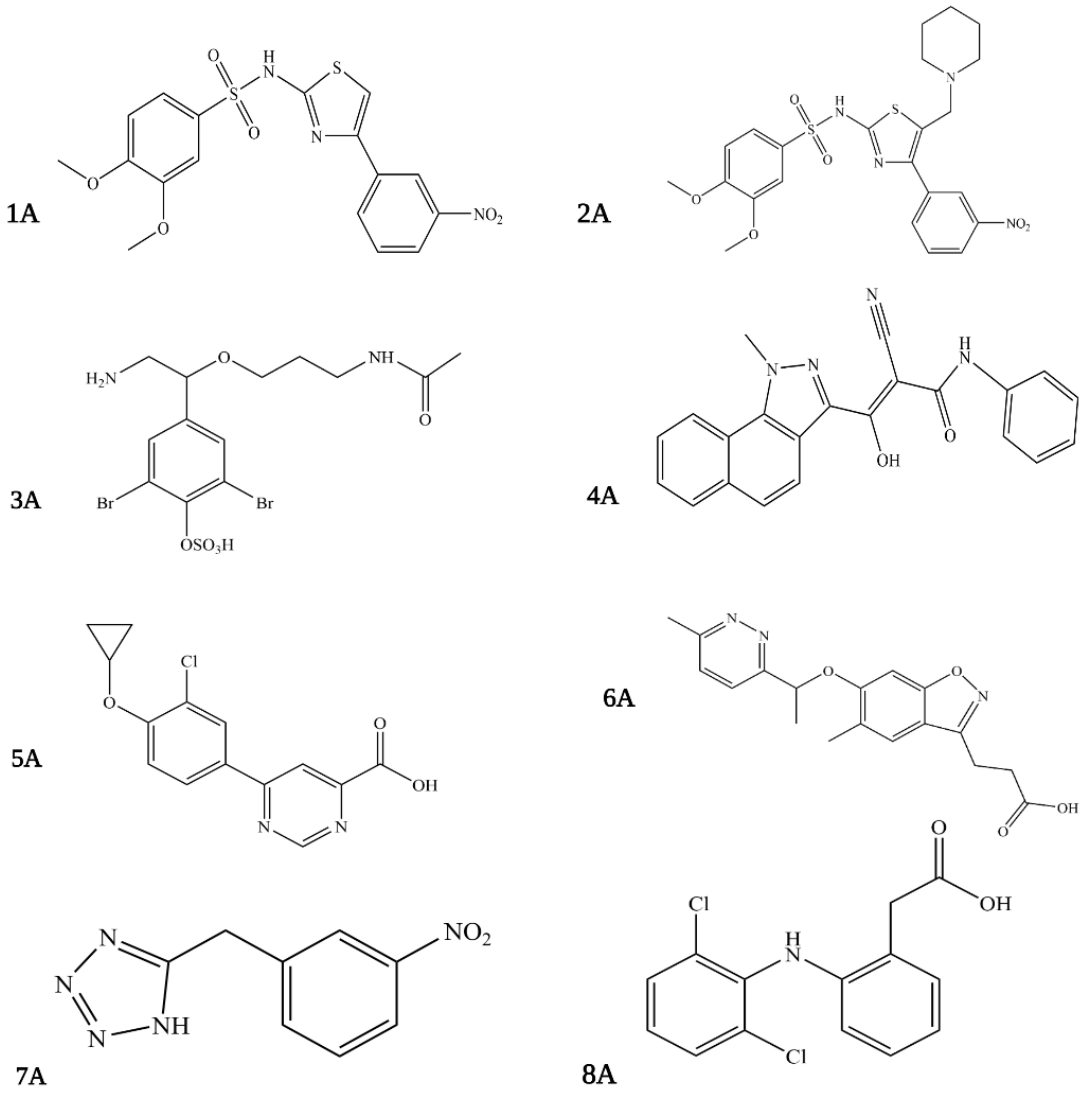

Figure 1.6. A schematic overview of non-substrate analogs KMO inhibitors.

Limitations

Though substrate analogs show inhibition, some of them have shown the potential of causing life-threatening side effects since they were found capable of generating cytotoxic hydrogen peroxides through flavin reduction. Upon binding, NADPH reduces FAD and leaves as $NADP^+$, then the oxygen molecule binds and forms the L-kyn -FAD-hydroperoxide complex intermediate. The oxidation of L-kyn proceeds to make water and 3-HK. Since these compounds have similarities to L-kyn, it has been observed that some potential KMO inhibitors are rather uncouplers of NADPH instead of KMO inhibitors [54]. In the presence of m-NBA and UPF-648, the accumulation of peroxy flavin decay has been observed to yield hydrogen peroxide without hydroxylation [54, 63].

A most recent study [63] provided a better understanding of how uncoupling happens. They proposed the flavin reduction in KMO is due to conformational changes via π- π interactions between a substrate of an NADPH uncoupler and the loop above the re side of the flavin. They determined that the substrate-binding precedes flavin reduction. Ro 61-8048 has shown interesting results where it acts as a competitive inhibitor in sc and hKMO and an NADPH uncoupler in pfKMO. This is due to the different binding modes this compound has in those two species. It binds in the active site of scKMO but does not induce conformational changes in the protein chain the same way it does in pfKMO. All this considered, it is imperative to assess the generation of hydrogen peroxides in making more potential KMO inhibitors in the future.

Our compounds

In this study, we have proposed and examined several KMO binders in efforts to find treatment for neurodegenerative diseases. We have deduced these compounds using structure-activity relationship (SAR), receptor-based pharmacophore modeling as well as molecular similarity techniques.

The second chapter of my dissertation presents the synthesis and biochemistry studies of a kynurenine analog, 5-Nitrokynurenine (5-NKyn). This compound is structurally similar to mNBA[64], one of the first kynurenine analogs to be proposed and evaluated for KMO inhibition. As previous studies have shown, the binding of a ligand to KMO no matter how tight does not always guarantee the KMO inhibition that is therapeutically desired. Therefore, though we show that this compound binds to KMO and inhibits the hydroxylation of kynurenine, it does this by uncoupling NADPH, a phenomenon that is thought to lead to an eventual accumulation of hydrogen peroxides [54], an undesirable side effect. Therefore, though it prevents product formation, more modification of its structure is needed to prevent this side effect.

The second class of our proposed compounds is multitargeting compounds capable of inhibiting enzymes on KP that are involved in free radical generation simultaneously. This approach is the most suitable for multifactorial diseases such as neurodegenerative diseases and cancer in which their etiologies consist of more than one entity [7, 9]. In the third chapter, we evaluated a known kynureninase inhibitor: SAPCO for KMO inhibition. We observed a tight binding to KMO which, unlike 5-NKyn, was able to inhibit KMO without uncoupling NADPH thus making it a better lead candidate for neurodegenerative diseases treatment.

The third class of KMO inhibitors we proposed are tertiary sulfonylureas. These compounds were previously computationally predicted and evaluated for NOX inhibition. There is much therapeutic relevance of inhibiting NOX such as decreasing the accumulation of reactive oxidative species (ROS) and their role in cardiovascular diseases. Surprisingly, these compounds were computationally predicted to bind and inhibit KMO as well. Given the multifactorial nature of neurodegenerative disorders, the concept of "one target, one drug" is not efficient in treatments of such disorders [7] therefore, finding a small molecule that can simultaneously inhibit two enzymes that have a major role in oxidative stress, would ensure maximum therapeutic benefits towards neurodegenerative disorders.

Last but certainly not least, are phenylalkanoic acid NSAIDS and their derivatives. Again, using the same pharmacophore that predicted our sulfonylureas, PAA-1 was initially predicted to inhibit KMO. Among all our previously proposed ligands, PAA-1 had the best inhibitory potency. However, the structural similarities of these compounds to commercially available and FDA-approved NSAIDs lead us to propose Fenbufen and other derivatives for KMO inhibition. And indeed, the results were very encouraging. There are a lot of advantages to this finding, given that these compounds already have FDA approval, they are thus the best lead candidates in our library.

CHAPTER 2

SYNTHESIS OF 5-NITROKYNURENINE AS A POTENTIAL INHIBITOR OF *CYTOPHAGA HUTCHINSONII* KYNURENINE MONOOXYGENASE

Emma Carine Iradukunda, Thomas Kizzar and Robert S. Phillips. To be submitted *to the Organic & Biomolecular Chemistry Journal.*

ABSTRACT

Kynurenine Monooxygenase (KMO) is a potential drug target for neurodegenerative diseases such as Alzheimer's disease and Huntington's disease. Given the therapeutic relevance of KMO inhibition, we synthesized a 5-Nitrokynurenine (5-Nkyn) and tested it for competitive inhibition of KMO. We observed a high blank rate in reactions with 5-Nkyn as expected for non-substrate effectors of KMO; this phenomenon leads to the accumulation of hydrogen peroxides, a life-threatening side effect. In addition, though 5-Nkyn maintained the charge-to-charge interaction with Arg-83 as expected of kynurenine analogs, the compound exerts an overall different binding mode. These results indicate that substituting kynurenine with a nitro group on the para position deactivates the ring and therefore leads to the uncoupling of NADPH.

INTRODUCTION

Over the past two decades, kynurenine monooxygenase (KMO) has been of great therapeutic interest because of its involvement in defining the balance between N-Methyl-D-aspartic acid (NMDA) receptor agonism and antagonism [65]. Furthermore, the hydroxylation of kynurenine (L-kyn) by KMO (Figure 2.1) is the entry point to the synthesis of two free radical generators: 3-hydroxykynurenine (3-HK) and 3-hydroxyanthranillic acid (3-HAA) [66, 67], and an NMDA receptor agonist, quinolinic acid (QA) [39, 40, 68, 69]. KMO inhibition has therefore emerged as a therapeutic target for neurogenerative disorders such as Alzheimer's (AD), Huntington's (HD) and Parkinson's (PD) diseases[41, 58]. KMO inhibition not only eradicates the production of the above neurotoxic metabolites, but it also promotes increased production of a neuroprotectant NMDA receptor antagonist [70]: Kynurenic acid (KA), via kynurenine aminotransferase (KAT). Since KMO and KAT share the same substrate, the inhibition of KMO increases the bioavailability of L-kyn which in turn leads to neuroprotection as it increases the levels of KA in the brain. Chronic oral administration of a KMO inhibitor, JM6, in a transgenic mouse model of AD reduced extracellular glutamate owing to the increase of KA levels in the brain. KMO inhibition also results in the amelioration of HD symptoms in a mouse model [58]. Brain changes associated with Alzheimer's diseases such as high-affinity to choline and a significant decrease in cortical choline acetyltransferase were observed when QA was introduced in the nucleus basalis of rats; however, when KA and QA were co-injected, no such changes were suggesting that KA protects the brain against damages caused by QA neurotoxicity[70]. The paradoxical importance of these enzymes led us to synthesize and purify 5-nitrokynurenine (5-NKyn, Figure 2.2); a kynurenine analog, with the potential to inhibit *Cytophaga hutchinsonii* KMO (chKMO)

and thus shift the pathway towards neuroprotection. (m-Nitrobenzyl)alanine (m-NBA), the desamino analog of 5-NKyn, was shown previously to inhibit KMO in rats[43].

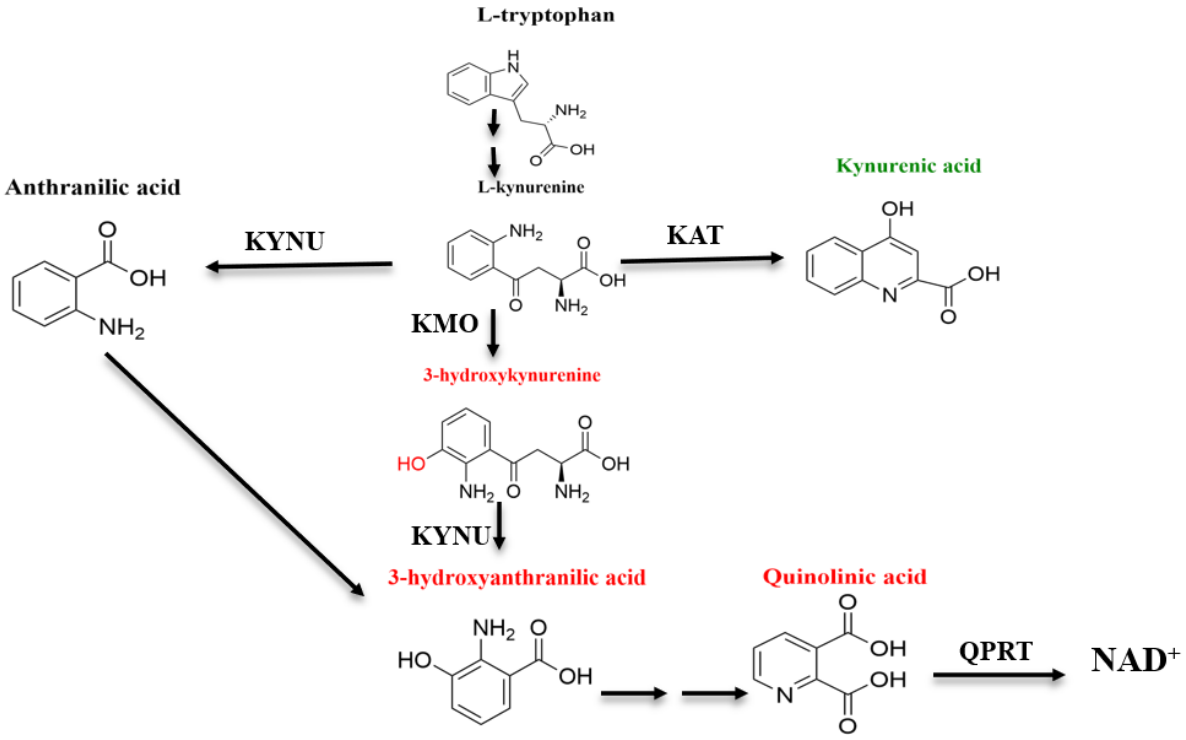

Figure 2.1. Schematic overview of kynurenine pathway highlighting metabolites involved in neurotoxicity (red labels) and neuroprotection (green label).

Figure 2.2. A structure of our proposed KMO ligand: 5-NKyn **(A)** in comparison to m-NBA **(B).**

Kynurenine analogs were the first set of KMO ligands to be examined for competitive inhibition [71,57, 55]. Given their structural similarities with the physiological substrate, they often bind to the active site with greater affinity than L-kyn and competitively inhibit KMO. Both structure-activity relationships (SAR) [59] and crystallographic [1] studies had shown that the key requirement for KMO inhibition is: 1) The aromatic moiety to occupy the hydrophobic region in the active site; and 2), approximately three spacer atoms between the aromatic region and the carboxylic acid moiety to maintain the charge-charge interaction with a conserved Arginine residue in the active site. The SAR study [59] revealed that strong binding does not need the amino group to be present on the ligand. Since KMO is an NADPH-dependent flavoenzyme, substrate-like inhibitors can stimulate FAD reduction of dioxygen without going through hydroxylation as expected for monooxygenases, a phenomenon that leads to the accumulation of hydrogen peroxides [54 63].

MATERIAL AND METHODS

Growth of *E. coli*-containing plasmids. chKMO[72] was expressed in *E. coli* BL21 (DE3). A single colony grown on LB/kanamycin agar plates was removed and transferred to 5 ml of sterile LB broth with 5 µl kanamycin overnight at 37 °C with shaking at 180 rpm. That overnight culture was then added to separate 1 L flasks containing 1 L Studier autoinduction [73] medium supplemented with 200 mg/L kanamycin. The cells were grown at 37 °C for 24 hours with shaking (220 rpm). Cells were then collected by centrifugation for 15 minutes at 4000 rpm at 4 °C and stored at -80°C until used for enzyme purification.

Purification of chKMO. Cells were resuspended in 30 ml 0.05M Tris-acetate buffer supplemented with 1 mM DTT, 0.2% Triton X-100, and 5 µM FAD. The yellow suspension was sonicated on ice in 4 60-second bursts with 3 minutes cooling between bursts. Debris was removed by centrifugation for 1 hour 30 minutes at 4000 rpm at 4 °C.

Nickel column chromatography. The enzyme solution from the previous step was loaded on the Ni-chelate column equilibrated with 0.05 M Tris-acetate buffer (pH 8.0, 5 µM FAD, 0.5 mM DTT), followed by washing with 100 ml 0.005M Tris-acetate buffer (PH 8.0, 5 µM FAD, 0.5 mM DTT, 20 mM imidazole) buffer. The protein was eluted using 0.05 M Tris-acetate buffer (0.2 M mannitol, 0.2% Triton X-100, 5 µM FAD, 1 mM DTT, 200 mM imidazole, pH 8.0). The fractions that possessed a brilliant yellow color and contained significant KMO activity (steady-state observations section) were pooled and concentrated using a centrifugal concentrator (30 kDa cutoff) at 4 ºC for 1 hour 3 times using the exchange buffer (0.05 M Tris-acetate buffer pH 8.0, 5 µM FAD, 0.5 mM DTT).

Diethylaminomethyl column (DEAE). For further purification, the protein was loaded onto a DEAE-Sepharose column (30 cm · 2.5 cm) pre-equilibrated with the same buffer used for the Ni-NTA column, followed by washing with the same buffer with 20 mM NaCl. The protein was eluted overnight using 0.05 M Tris-acetate buffer and 200 mM NaCl. The fractions that possessed a brilliant yellow color and contained significant KMO activity were pooled and concentrated using a centrifugal concentrator (30 kDa cutoff) at 4 ºC for 1 hour 3 times using the exchange buffer (0.05 M Tris-acetate buffer pH 8.0, 5 µM FAD, 0.5 mM DTT). This was then distributed into several Eppendorf tubes, flash-frozen with liquid nitrogen, then stored at -80°C.

Protein determination. The concentration of purified chKMO was determined using a Cary 1E UV-Vis spectrophotometer with a quartz cuvette of path length 1 cm. The concentration of chKMO was obtained by a scan between 400-200 nm for a solution of 10 µL protein and 10 µL 1M potassium phosphate, pH 7.0, in 380 µL of water. The concentration was calculated using the Beer-Lambert law using the molar absorbance for flavin at 450 nm (12,300 M^{-1} cm^{-1}).

Steady-state kinetics. The enzyme activity was determined by monitoring the NADPH consumption at t340 nm. The reaction mixture consisted of 530 µl of buffer (0.05 M Tris-acetate, pH 8.0, 1 mM DTT, 5 µM FAD), 6 µl 10 mM kynurenine, 10 µl 12 mM NADPH, 4 µl 1.5M KCl. The reaction was initiated by the addition of 50 µl of enzyme sample (21.6 µM). Kinetic parameters were determined by initial velocity measurements at a fixed concentration of NADPH (0.5 mM) and varying concentrations of kynurenine. For the enzyme inhibition assays, the above procedure was applied with varying concentrations of the compound H. The inhibitor constant (Ki) values were obtained using Compo software [74].

High-performance liquid chromatography. The reaction of compound H was measured by following the product formation using a Nucleosil 120-5 C-18 silica gel column from Machery-Nagel. The reaction mixture consisted of 100 µl reaction buffer (0.05 M Tris-acetate, pH 8.0, 1 mM DTT, 5 µM FAD, 50 µM kynurenine) 100 µM NADPH, 4 µM KMO, (0-100 µM) of Nitrokynurenine. Elution was in 0.1% acetic acid/5% methanol for 5 minutes, then a gradient from 5% methanol to 70% methanol at 25 minutes was applied. The data were analyzed using Microsoft excel.

Synthesis of 5-Nitrokynurenine. Lithium nitrate (0.090 g, 1.3 mmol) and 0.10 g N, N-diacetyl-L-kynurenine methyl ester (0.33 mmol) was added to 2 mL trifluoroacetic acid, with stirring. Then, 0.137 mL H_2SO_4 (2.46 mmol) was added, and the orange solution was stirred at room temperature for 4 hours. TLC (silica gel, EtOAc) showed that the starting material was gone, so 5 mL water and 0.12 g urea were added, and the mixture was refluxed overnight. The reaction mixture was then cooled, treated with charcoal, and filtered through Celite. The filtrate was added to 11 g Dowex-50-X8 (H^+) and filtered. The resin was washed with water until the washings were colorless. The product was then eluted with 80 mL 1M NH_3. The orange filtrate was evaporated in vacuo, and the residue was triturated with acetone. The precipitate was filtered and dried, giving 0.033 g (39.5%) of a red-orange solid. NMR (DCl in D_2O, δ = 8.61 (1H, d, J=2.4 Hz, H-6), 7.99 (1H, dd, J=2,4, 9.1 Hz, H-4), 6.72 (1H, d, J=9.4 Hz, H-3), 4.40 (1H, t, J=4.5 Hz, α-H), 3.82 (1H, dd, J=5.3, 19.0 Hz, β-H), 3.76 (1H, dd, J=4.2, 19.5 Hz, β-H). MS: m/z=253.2 (need to get the real number). UV, (need to insert spectral details, λ_{max} and ε).

RESULTS AND DISCUSSION

KMO inhibition is currently an active area of study in the discovery of a breakthrough drug for various neurological disorders. KMO is an NADPH-dependent flavoenzyme that catalyzes the hydroxylation of L-kyn to 3-HK. Among the proposed KMO inhibitors, kynurenine analogs have shown the potential to bind tightly to KMO with different binding modes that could result in KMO inhibition, substrate-like behavior, or uncoupling of NADPH without hydroxylation. Kynurenine analogs with halogen substitution on C-5 are known to be excellent substrates of KMO suggesting that with proper modification, they could serve as potential lead inhibitors of KMO (reference?). In this study, we synthesized a novel kynurenine analog and tested it for

KMO binding affinities. The synthesis of 5-NKyn was unexpectedly challenging. The reaction of protected kynurenine under standard nitration conditions (HNO_3:H_2SO_4, 1:1) resulted in the unreacted starting material. This is most likely due to the protonation of the substrate in the strongly acidic medium resulting in deactivation. Under more severe conditions, KNO_3 in H_2SO_4, nitration proceeded, but there were several products detected by TLC. Hence, we tried a less acidic solvent, trifluoroacetic acid, with $LiNO_3$ and stoichiometric H_2SO_4. This condition resulted in a rapid reaction to form a single product by TLC. Hydrolysis of the protected nitrokynurenine was performed without isolation of the initial product, giving the desired 5-nitrokynurenine isolated in modest yield.

Our interest in 5-Nkyn is based on the reaction mechanism of KMO[54]. Our initial hypothesis was that 5-NKyn can act as either an inhibitor, a substrate, or a non-substrate effector of KMO, like most other kynurenine analogs[54, 56]. We observed a high blank rate in inhibition assays in the presence of 5-Nkyn, which suggested that it could be either an uncoupler of NADPH oxidation or a potential KMO substrate as observed in other kynurenine analogs with substitution of C-5[56]. Given that the third position on the ring was still open, we thought that 5-Nkyn could be acting as a substrate of KMO. However, using HPLC, we did not observe a new peak with absorbance around 370-400 nm as expected for when hydroxylation of kynurenines occurs [56,1] (Figure 2.3). Hence, 5-Nkyn was indeed consuming NADPH without hydroxylation, a phenomenon associated with the accumulation of highly toxic oxygen species[54, 63]. Another structurally similar nitro-containing KMO ligand m-NBA (see Figure 2.2) had already been shown to act as both inhibitor or a substrate effector of KMO depending on the enzyme specie[63].

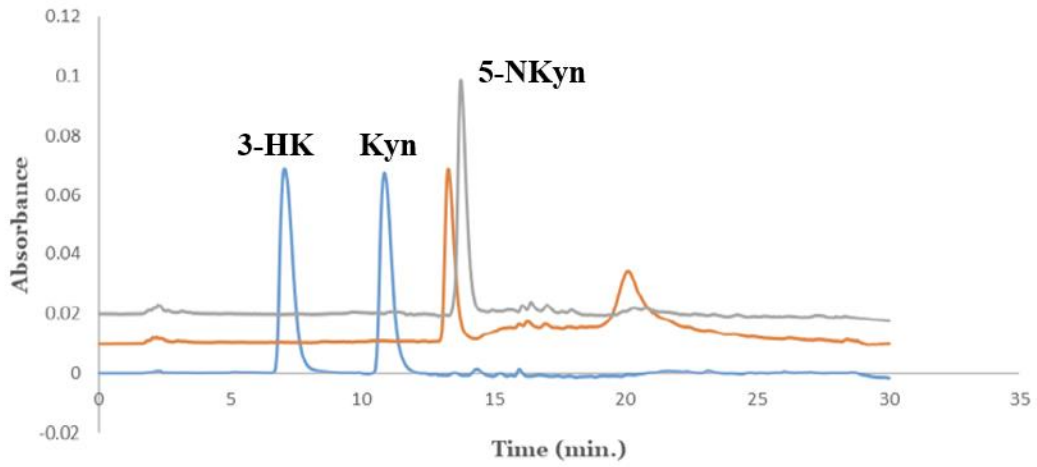

Figure 2.3. HPLC analysis of 5-NKn reaction with KMO-orange line; black line: control; blue line reaction of kynurenine with KMO.

Using Autodock Vina, we followed the protocol proposed and validated by Amaral [1], Toledo-Sherman[60]and Steven[62] to assess the binding mode of this compound. As expected for KMO binders[1, 63], 5-Nkyn interacted with the conserved Arg 83 residue in the active site via its carboxylate moiety (See Figure 2.4). As expected for KMO binders, the benzene ring occupies the hydrophobic pocket close to the FAD binding site, where the nitro group forms hydrogen bonds with FAD and a water molecule. A different mode of binding was most likely what caused the lack of the reactivity for the mechanism and resulted in uncoupling. A previous study suggests that halogen substitution on C-5 on a kynurenine analog serves as an excellent substrate of KMO. 5-Chlorokynurenine was the most potent among ligands tested with K_m about 3-fold lower than that of L-kyn [56]. Though 5-Nkyn acted as an uncoupler, our data shows that it still binds tighter than L-kyn (13± 6.1 µM), the lack of reactivity of 5-Nkyn can be attributed to the fact the nitro group is too deactivating compared to halogens.

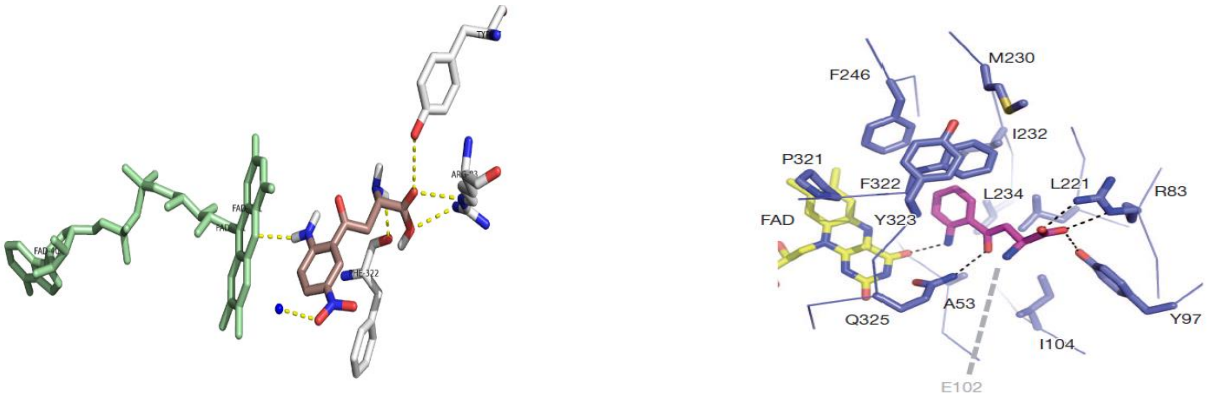

Figure 2.4. Active site of yeast KMO (pdb code: 4j36) in complex with 5-NKyn. Structure of L-kyn bound to yeast KMO (pdb code: 4j36) [1].

Conclusion

In this study, we present the novel synthesis of 5-NKyn and its inhibition potential using biochemical KMO inhibition and binding assays. We were able to nitrate kynurenine using $LiNO_3$ and H_2SO_4 in trifluoroacetic acid. Our kinetic studies show that this compound uncouples NADPH without hydroxylation, a process that triggers the accumulation of hydrogen peroxides. Previously, kynurenine analogs with substituents on C-5 have been shown to act as substrates of KMO. The lack of reactivity with 5-NKyn can be attributed to the strongly deactivating nature of the nitro group. The autodock data showed a different binding mode than L-kyn which supports the conclusions from the steady-state kinetic analysis. Nonetheless, 5-NKyn binds to chKMO with greater affinity than L-kyn suggesting that with further modification it can serve as a lead compound for neurodegenerative disorders.

CHAPTER 3

(*S*-(2-AMINOPHENYL)-L-CYSTEINE S, S-DIOXIDE INHIBITS BOTH KYNURENINE MONOOXYGENASE AND KYNURENINASE

Emma Carine Iradukunda* and Robert S. Phillips. To be submitted *to the Bioorganic & Medicinal Chemistry Letters.*

Abstract

The high oxygen (O_2) utilization rate of the brain vs the antioxidant availability makes the central nervous system (CNS) more vulnerable to the overproduction of free radicals leading to oxidative stress (OS). Kynurenine monooxygenase (KMO) and kynureninase (KYNU) not only share the same physiological substrate, kynurenine (KYN) but are also free radical generators. In this study, we examined (*S*)-(2-aminophenyl)-L-cysteine *S*, *S*-dioxide (SAPCO), a known KYNU inhibitor for competitive inhibition of *Cytophaga hutchinsonii* (ch) KMO. SAPCO was found to inhibit chKMO in the micromolar range providing a new lead compound for the treatment of neurodegenerative disorders. This study shines light on the multitargeting potentials of kynurenine analogs towards finding treatment for neurodegenerative disorders.

Background

Kynurenine (KYN)/L-kyn, on the kynurenine pathway (KP) (Figure 3.1), is a precursor of neuroactive metabolites, such as kynurenic acid (KA), quinolinic acid (QA), 3-hydroxykynurine (3-HK), and 3-hydroxyanthranillic acid (3-HAA). Thus, some enzymes on the KP are therapeutic targets for neurogenerative disorders such as Alzheimer's, Parkinson's, and Huntington's diseases [1-5]. KYN is at the key point of the KP and is a substrate of three enzymes: KYNU, KMO, as well as kynurenine aminotransferase (KAT). KMO hydroxylates KYN to 3-HK; KYNU then catalyzes the conversion of 3-HK to 3-HAA. 3-Hydroxyanthranilate dioxygenase (3HAO) catalyzes the oxidative ring opening to form 2-amino-3-carboxymuconate semialdehyde, which spontaneously cyclizes to form QA. KYN, though it is a weak substrate of human KYNU [6], hydrolyzes through its action to make anthranilic acid (AA) which oxidizes to make 3-HAA through the action of anthranilate 3-monooxygenase. Lastly, KYN converts to kynurenic acid (KA), catalyzed by KAT.

KYN is paradoxically a precursor to both neurotoxic and neuroprotective metabolites[7, 8]. For instance, both QA and KA regulate the N-methyl-D-aspartate receptor (NMDAr). QA is a known NMDAr agonist[9]; the overexpression of KP enzymes, especially KMO, results in the overproduction of QA which leads to the overflow of calcium into the NMDAr channel resulting leading to neuron damage. KA, on the other hand, exerts neuroprotective properties by antagonizing the NMDAr [10]. Research shows that KA protects the brain from the damages done by QA [11]. 3-HK and 3-HAA are free radical generators[12] that lead to the accumulation of reactive oxygen species (ROS) and oxidative stress (OS) in the central nervous system (CNS). OS is a known phenomenon in etiologies of neurodegenerative disorders because of its involvement in the initiation and progression of neuron damage.

KMO is at the critical point of KP, and its inhibition has proven to be therapeutically beneficial to neurodegenerative diseases. For example, several KMO inhibitors, such as Ro61-8048, and *m*-NBA, reportedly alleviated symptoms of neurodegeneration in mice models [13-15] and increased the availability of L-kyn and KA leading to neuroprotection [16]. However, KYNU catalyzes the conversion of L-kyn to AA, which subsequently is hydroxylated to 3-HAA, and later to the production of QA[17]; thus, simultaneous inhibition of KYNU and KMO inhibition would not only halt the synthesis of neuron damaging metabolites but also shift the pathway to the formation of KA, hence, restoring the antagonistic and agonistic NMDAr homeostasis.

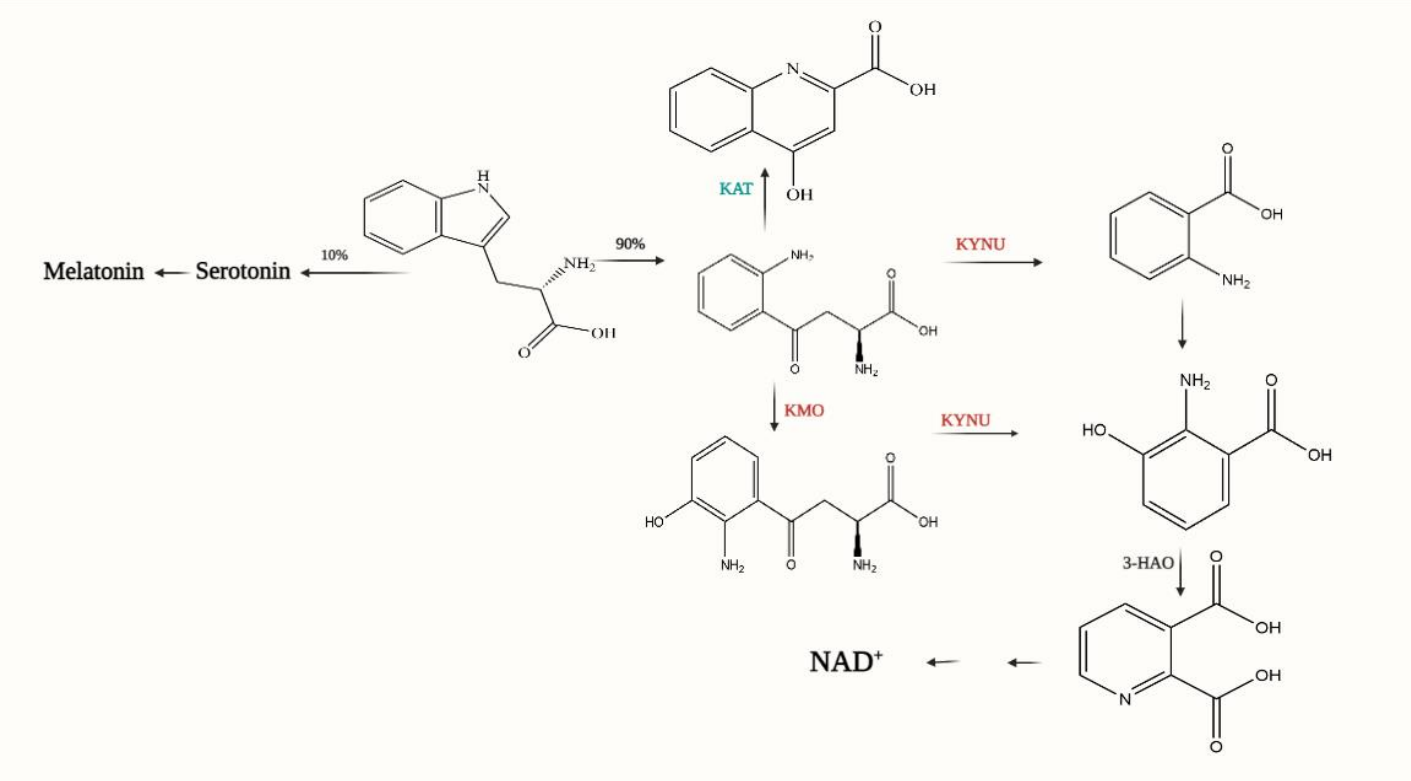

Figure 3.1. Kynurenine pathway highlighting enzymes that are involved in producing neuroactive compounds.

It was previously recognized that for better KMO inhibition, the electrostatic interaction between the arginine residue in the active site with a carboxylate or its bio-isostere was essential. Also, a hydrophobic moiety, a hydrogen bond acceptor, as well as three carbon spacers between the hydrophobic center and the acidic center, are needed on the ligand for a tighter binding. Substrate analogs such as *m*-nitrobenzoyl alanine (m-NBA) [14], (R, S)-3,4- dichlorobenzoyl alanine [18], and 3,5-dibromokynurenine [19] have all shown an appreciable inhibitory potency towards different species of KMO. Considering that both KMO and KYNU share the same substrate, KYNU inhibitors that meet the above-mentioned criteria can potentially inhibit KMO as well. Thus, we examined (*S*)-(2-aminophenyl)-L-cysteine *S*, *S*-dioxide (SAPCO, Figure 3.2), a kynurenine analog known to competitively inhibit KYNU [20], for KMO inhibition. This study explores the binding potency and binding modes of this compound and shines light on the multitargeting behaviors of kynurenine analogs.

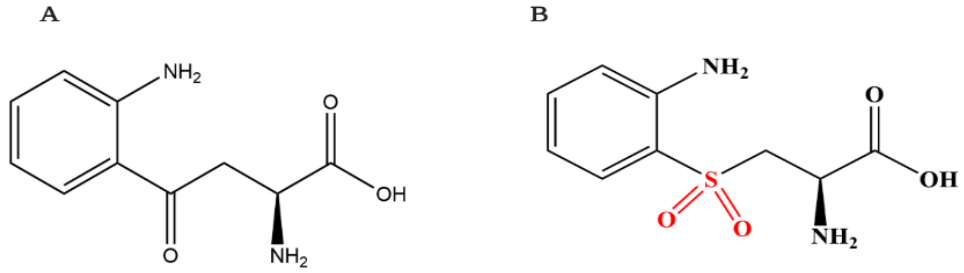

Figure 3.2. Structure of L-kyn (A) and SAPCO (B)

KMO is an NADPH-dependent flavoenzyme. The first step in the catalytic mechanism of KMO involves the binding of KYN to the KMO.FAD complex; next, NADPH binds to the complex to reduce the FAD and leaves as $NADP^+$. This step is followed by the binding of molecular oxygen

to the ligand-KMO-FAD complex to form a hydroperoxide intermediate followed by release of product and a water molecule[54].

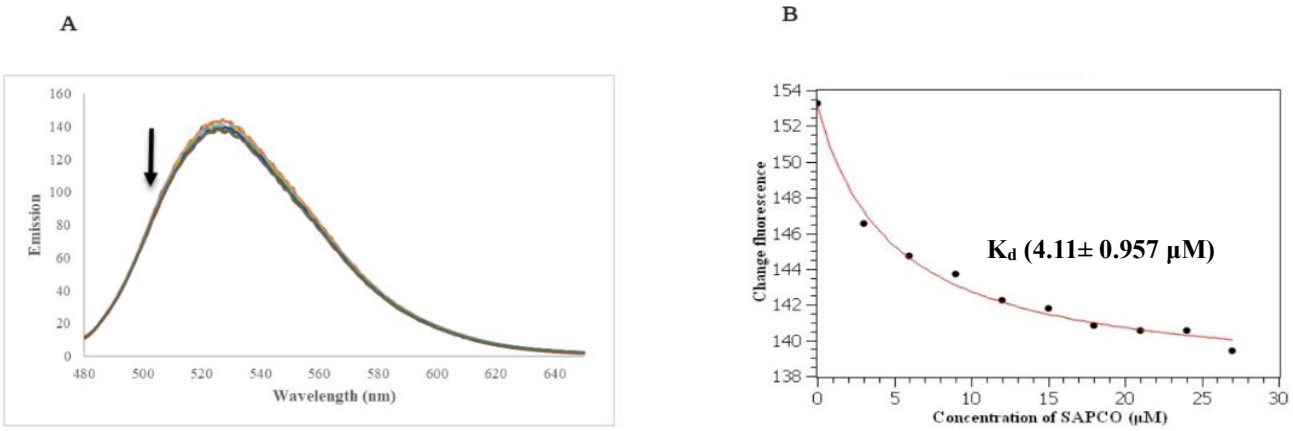

Figure 3.3. (A) Fluorescence quenching in the titration of 1µM KMO.FAD with SAPCO (0–27µM). (B) Change in FAD fluorescence versus free SAPCO.

The binding of a ligand to the KMO.FAD complex causes perturbance in the FAD fluorescence until the active site is fully saturated. Therefore, the change in FAD fluorescence at the wavelength of 520nm (FAD emission) can be used to measure the dissociation constant (K_d). For this study, we have measured the binding affinity using the method described by Moran et al. [21].

Results and discusion

For this study, SAPCO was titrated to the enzyme/buffer solution until it reaches saturation (Figure 3.3 A). The binding affinity was measured from the change in fluorescence (Figure 3.3. B) and our data show a significantly tighter binding (K_d = 4.11± 0.96 µM) compared to its analog L-kyn (K_d = 67 ± 15 µM) [19].

On the other hand, though kynurenine analogs similar to SAPCO have shown a very appreciable inhibitory potency towards KMO, many have been reported to cause the NADPH uncoupling [22]

[23] which leads to the accumulation of hydrogen peroxide, a less desirable side effect of the compounds. Therefore, to confirm that SAPCO was indeed inhibiting KMO without uncoupling NADPH, we measured the decrease of NADPH absorbance at 340 nm using the Cary 1E UV-vis spectrophotometer (data not shown). The lack of a high blank rate during this measurement suggests that SAPCO binds to KMO not as a substrate or an NADPH uncoupler, but as a competitive inhibitor.

Next, we were interested to get insights into how SAPCO binds to the active site of KMO. However, since the structure of chKMO is still unknown we turned to molecular modeling using a plugin for PYMOL, Autodock Vina and we used yeast KMO (PDB code 4J36) as our docking model since all the residues involved in the binding of the substrate are all conserved across both species (Figure 3.4) [19], following the protocol described in Seeliger et al. [24].

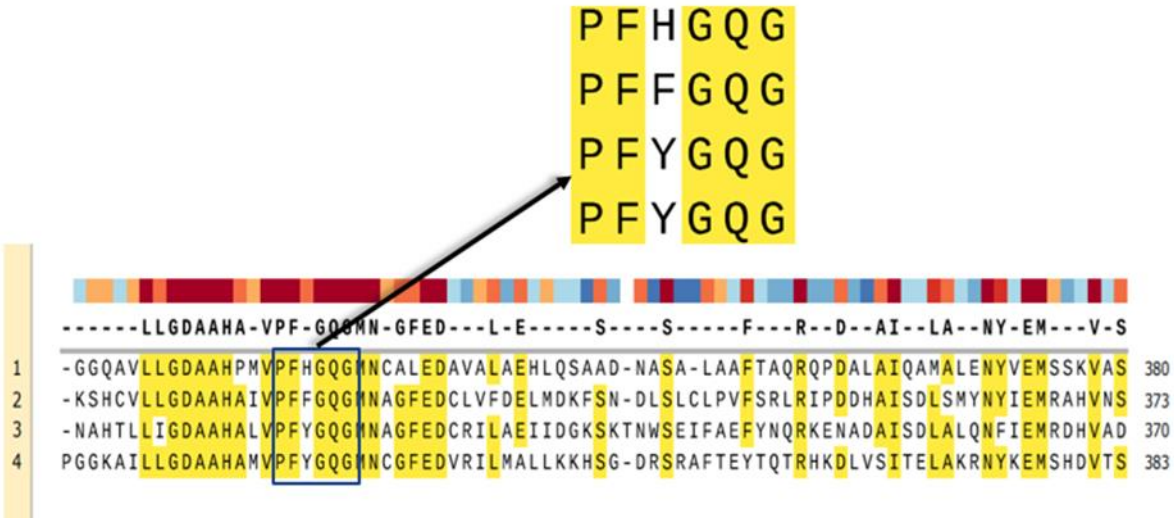

Figure 3.4. Sequence alignment of commonly used KMO species (1*: Pseudomonas fluorescens* KMO, 2: *human* KMO, 3: *Cytophaga hutchinsonii* KMO, 4: *Saccharomyces cerevisiae* KMO). The conserved active residues are highlighted with yellow color.

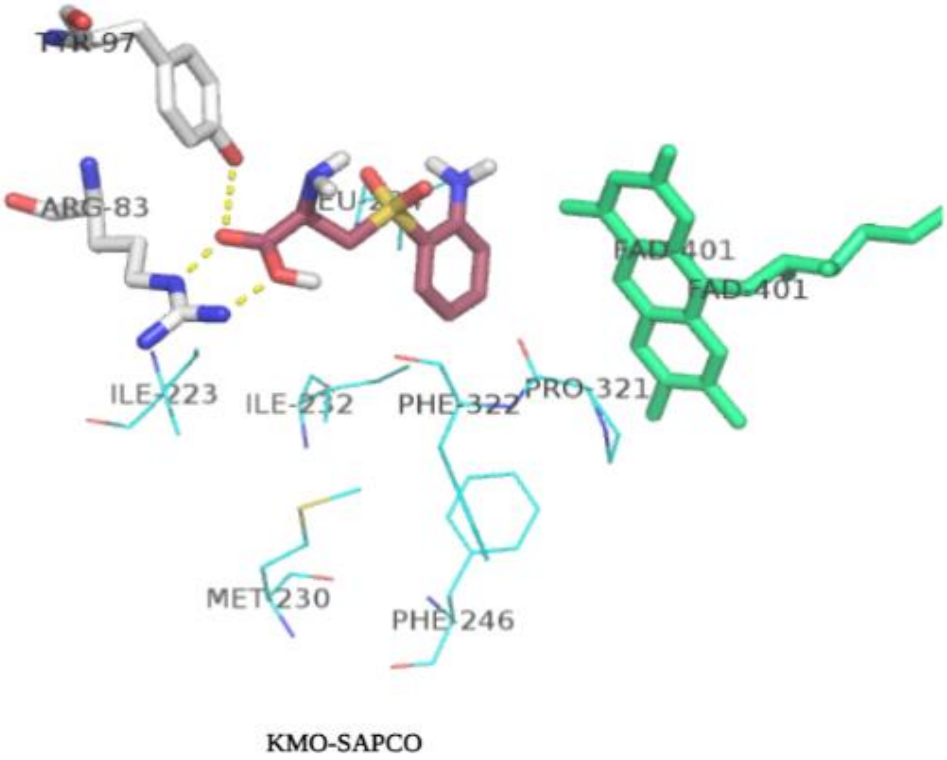

Figure 3.5. scKMO (PDB code: 4J36) in complex with FAD cofactor (green) bound to SAPCO (raspberry red).

We notice that SAPCO made polar contacts with Arg 83 and Tyr 97 via its carboxylate (Figure 3.5). The aromatic ring also occupied the hydrophobic pocket facing the *re*-side of FAD like KYN. Though the role of the carbonyl group on KYN is not thoroughly researched, replacing it with a sulfonyl group as in SAPCO resulted in an overall tighter binding of SAPCO to KMO.

Conclusions

We have demonstrated that SAPCO, a known competitive inhibitor of KYNU, also inhibits KMO in the lower micromolar range. The ability for this compound to simultaneously inhibit

both enzymes is thought to not only halt the production of neurotoxic metabolite on the KP: 3-HK and 3-HAA and QA, but we also expect an increase in the KYN and KA availability in both plasma and brain which leads to neuroprotection. Though we have no experimental evidence that this SAPCO will be able to cross the blood-brain barrier (BBB), its resemblance to KYN leads us to hypothesize that it could be transported through the BBB by the large neutral amino acid carrier such as in KYN. Nonetheless, research shows that the inhibition of KMO in the periphery increases the bioavailability of KYN which readily crosses the BBB and thus increases the KA in the brain. Finally, more studies are needed to confirm the in vivo potency of this compound on both enzymes.

CHAPTER 4

EVALUATION OF TERTIARY SULFONYLUREAS NOX INHIBITORS FOR *CYTOPHAGA HUTCHINSONII* KYNURENINE MONOXYGENASE INHIBITION

Emma Carine Iradukunda and Robert S. Phillips. To be submitted *to the Bioorganic & Medicinal Chemistry Letters.*

Abstract:

The imbalance between the formation of reactive oxygen species (ROS) and its removal leads to oxidative stress (OS) in the central nervous system (CNS). The OS is known to contribute to the initiation and progression of neuron damage. The inhibition of enzymes involved in OS is thought to play a therapeutic role in neurodegenerative disorders especially Alzheimer's (AD), Parkinson's (PD), and Huntington's (HD) diseases. The two known enzymes that contribute to OS are nicotinamide adenine dinucleotide phosphate oxidase (NOX) and kynurenine monooxygenase (KMO). Therefore, this study takes a multitargeting/polypharmacological approach to evaluate three known NOX inhibitors predicted by our recently designed pharmacophore for KMO inhibition as a therapeutic resolution to various neurodegenerative disorders. Our data indicate that NOX inhibitors do indeed competitively inhibit the activity of KMO.

Letter:

It is widely known that neurodegenerative diseases are multifactorial and complex pathological conditions [75], in which mechanisms are not fully understood and involve multiple pathways and environmental factors. Even though neurodegenerative disorders such as Alzheimer's disease, Huntington's disease, Parkinson's diseases have distinctive symptoms, they all share common etiology and therefore, common biological targets. The four most common denominators in their etiology include oxidative stress[76, 77], accumulation of misfolded or unfolded proteins[18], dyshomeostasis of both redox-active metal ions such as copper and iron, as well as redox-inactive metal ions such as zinc [78-80], and finally, the abnormal function of the mitochondria[22]. Enzymes on the kynurenine pathway (KP) (Figure 4.1) such as KMO, kynureninase (KYNU) as well as kynurenine aminotransferase (KAT) catalyze reactions that lead to free radical generators: 3-hydroxykynurenine (3-HK) and 3-hydroxyanthranillic acid (3-HAA), as well as N-methyl-D-aspartate receptor (NMDAr) agonist and antagonists such as Quinolinic acid (QA) and kynurenic acid (KA) respectively. Kynurenine (KYN) is at the key point of the KP and paradoxically, it is a precursor for both the neuroprotective metabolite: KA, and the neurotoxic metabolites: 3-HK, 3-HAA, and QA. Therefore, inhibiting the activity of KMO had shown to not only inhibit the production of neurotoxic metabolites and cease the excessive OS but to also shift the pathway towards the production of more KA/neuroprotectant [81]. Several KMO inhibitors such as FCE288A [55] and Ro-61-8048 [57, 82, 64] have shown the potential of not only inhibiting KMO but also shifting the pathways towards the formation of more KA.

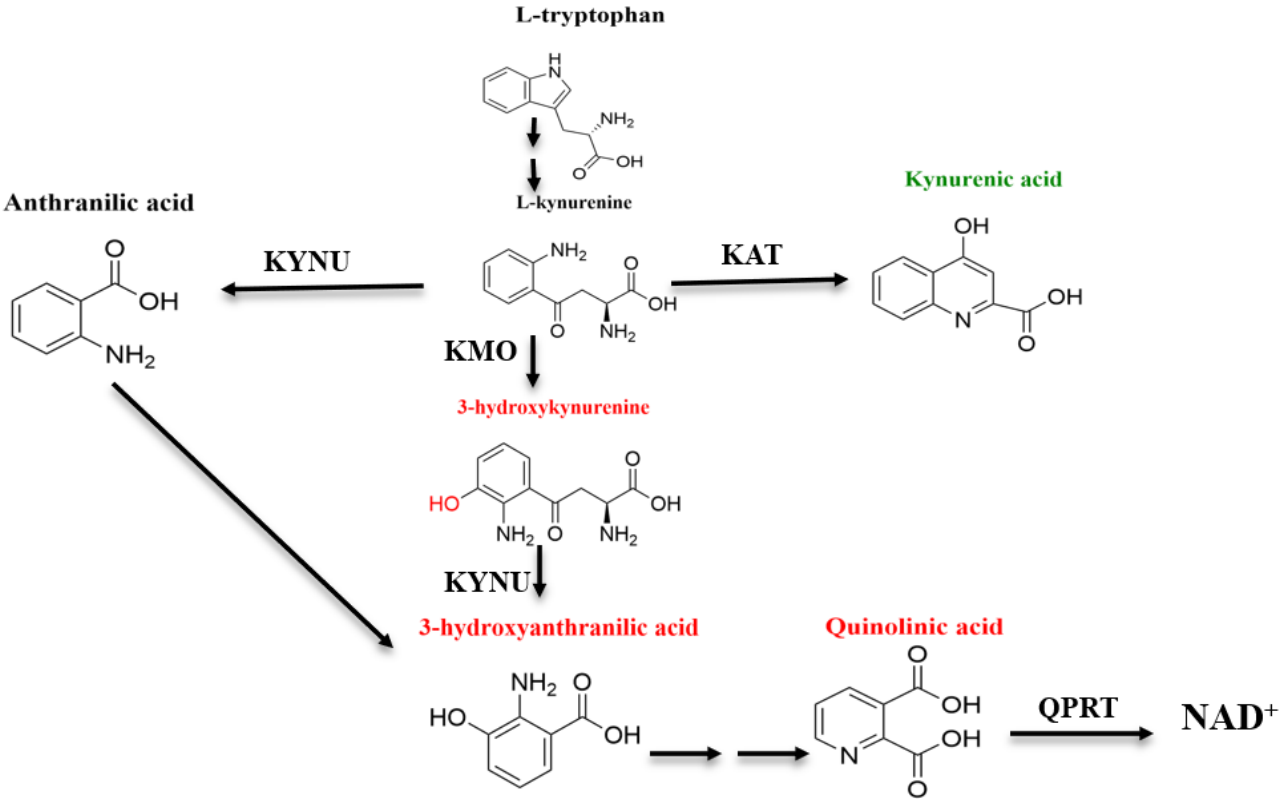

Figure 4.1. Kynurenine pathway. Green: neuroprotective metabolite, red: neurotoxic metabolites.

NOX on the other hand is an enzyme known to be activated during respiratory bursts where it generates superoxide responsible for animal immune response. The presence of ROS such as superoxide results in OS. Therefore, inhibiting NOX is therapeutically significant in the treatment of neurodegenerative diseases. A NOX inhibitor Diphenyleneiodonium (DPI) had for instance shown to be neuroprotective by reducing the up-regulation of NOX thereby reducing the OS[83]. An *in vivo* study showed a significant decrease of lipopolysaccharide injury within 24h when 1gm/kg/day of DPI was administered in rats[84]. Finally, the selective inhibition of NOX

with an ultralow dose of DPI significantly decreased microglia-mediated neuroinflammation and stopped the progression of Parkinson's disease in mouse models[85].

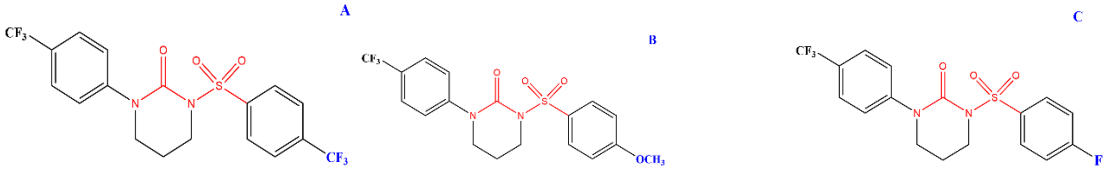

Figure 4.2. Structures of proposed sulfonylureas for KMO inhibition.

Using structure-based pharmacophore modeling[56], structure-activity relationship (SAR) [60,59], as well as drug repurposing[62]; hundreds of KMO ligands were proposed and evaluated as lead drug candidates of neurodegenerative diseases. In this present study, we propose three tertiary sulfonylureas A, B, and C (Figure 4.2) as potential KMO inhibitors deduced using our pharmacophore model. Surprisingly, these same compounds were predicted and evaluated as NOX inhibitors[86]. As noted earlier, neurodegenerative disorders are multifactorial, and as such, an ideal therapeutic approach would be the one that involves targeting more than one biological entity. The latter can be achieved through combination therapy and multitargeting drugs. As of 2017, 10% of the FDA-approved drugs were a therapeutic combination, and 21% of them were multitargeting drugs [75]. Multi-targeting drugs however have shown more therapeutic advantages over combination drugs given that combination therapy is often associated with incompatible pharmacokinetics and increased toxicity [87 8].

Results and discussion

A previous pharmacophore model was designed and predicted compounds A, B, and C as NOX binders, further biological studies revealed their different binding modes. The synthesis and characterization of these compounds are described in Qian Xu Et. Al. [86]. They all inhibit NOX in

the lower micromolar range (Table 4.1). A separate pharmacophore was generated using the Schrodinger package [88]and predicted the same compounds as potential KMO binders. This pharmacophore consists of four key components: hydrophobic centers, H-bond receptors, aromatic centers as well as the carboxylic acid the center. Though compounds A, B, and C lack the carboxylic center, they contain a sulfonylurea moiety which acts as a (bio)isostere for carboxylic acid. The carboxylic acid centers play a cardinal role in the inhibition of KMO as they maintain an essential electrostatic interaction via Arg 83 in the active site[1].

KMO is an NADPH-dependent flavoenzyme. The first step in the catalytic mechanism of KMO involves the binding of the substrate to the KMO-FAD complex, followed by the reduction of FAD by NADPH. The oxygen molecule then binds to produce the L-kynurenine-KMO-hydroperoxide complex which subsequently leads to the hydroxylation of L-kyn and the release of a water molecule. The binding of the substrate/ligand to the KMO-FAD complex results in the perturbation of the FAD fluorescence around 520nm [54]. We have therefore measured the dissociation constant (K_D) using the perturbation of the FAD fluorescence as described by Moran. Et. Al. and Amaral. Et. Al [1].

Although compounds A, B, and C are soluble in 100% DMSO, they precipitated as soon as they were added to the KMO reaction mixture consisting of 530 µl of buffer (0.05 M Tris-acetate, pH 8.0, 1 mM DTT, 5 µM FAD), 6 µl 10 mM kynurenine, 10 µl 12 mM NADPH, 4 µl 1.5M KCl. The reaction was initiated by the addition of 50 µl of enzyme sample (21.6 µM). As a result, particles in the cuvette scattered the incident light which gave a high noise and resulted in a huge error. We realized that KCl which is often used in KMO steady-state kinetic assays is not important for KMO enzymatic activity. We then removed it from our assays which improved the

solubility tremendously. Furthermore, we also noticed that using a room temperature buffer vs a "cold" buffer i.e., straight from a 4°C refrigerator keeps the reaction mixture from precipitating.

Compound	**NOX**	**chKMO**
	$IC_{50}(\mu M)$	$(K_d\ (\mu M)$
A (CF_3)	-	17+/- 5.4
B (OCH_3)	27	29.59+/- 3.9
C (F)	0.5	96.94+/- 32.54

Table 4.1: a comparison of inhibitory potencies of proposed tertiary sulfonylureas on NOX vs chKMO.

A PYMOL plugin, Autodock vina was used to further gain insights on how these ligands bind with KMO active site. However, since the structure of chKMO is not yet solved, we used the *saccharomyces cerevisiae* KMO (scKMO) as our docking model. scKMO was the first KMO species to be solved [1], it shares all the residues that make direct contact with the substrate in both chKMO and homo sapiens (h) KMO.

Our docking data shows that our sulfonylureas all adopt a conformational change in the active site to be in proximity with the active residues. Previous studies on KMO, both crystallographic and kinetic, highlighted that indeed the ligand's electrostatic interaction with Arg 83 is essential for a tighter binding of the compound to the active site [1]. There is also a conserved hydrophobic pocket across several known KMO species[1, 50] where the aromatic ring of the substrate is

situated. The latter consists of Leu 221, Met 230, Ile 232, Leu 234, Phe 246, Pro 321 ad Phe 322. However, unlike in L-kyn, our sulfonylureas have two aromatic centers instead of one. The presence of a non-aromatic six-membered ring allowed these compounds to bend at the sulfonylurea moiety resulting in lesser binding energy than when they bind linearly. Compound A (K_d:17 +/- 5.4 µM) which holds CF_3 on both benzene rings is the most potent among our proposed sulfonylureas. It kept the charge-to-charge interaction with Arg 83 via its carbonyl on the sulfonylurea moiety (see Figure 4.3). The two benzene rings holding CF_3 occupied the hydrophobic pocket as in L-kyn. The above observation corresponds with the literature, where research shows that the more fluorinated the inhibitor is, the stronger the binding of that ligand to the enzyme even when the fluorinated group does not interact with residues in the active site [89].

When the CF_3 group was replaced by methoxy in compound B, the binding affinity slightly reduced (K_d:29+/- 3.9 µM). The bending of compound B allowed it to make a weaker hydrogen bond with Arg 83 via its methoxy group and the rearrangements of active residues resulted in a new contact with Tyr 97 via sulfur dioxide on the sulfonylurea moiety (Figure 4.3).

Finally, we observed a much weaker binding affinity when the trifluoro group was replaced by fluoride in compound C (K_d: 96.94+/-32.54 µM). Replacing CF_3 with simply fluoride in compound C resulted in a weaker enzyme inhibition even though it still maintained the interactions with Arg83 and Tyr 97 (Figure 4.3). However, the hydrophobic pocket was not occupied making the inhibition weaker than the previous compounds. This highlights the importance on the binding affinity of the aromatic centers of our pharmacophore as well as their occupation of the hydrophobic pocket.

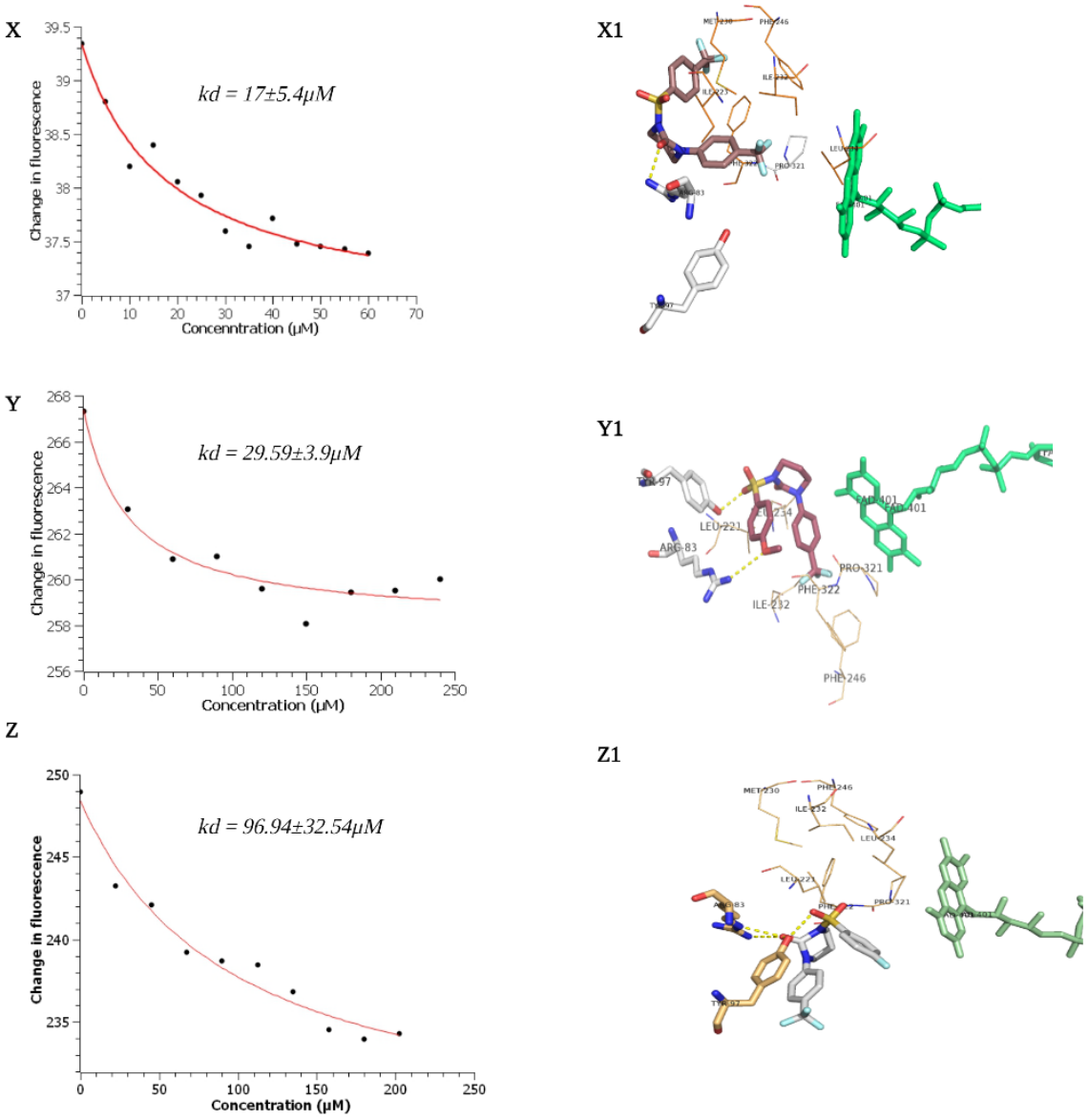

Figure 4.3. Left panel (X, Y, and Z): Binding affinities of compounds A, B, and C, respectively. Right panel (X1, Y1, and Z1) Active site of scKMO (PDB code: 4J34) in complex with compound A, B, and C, respectively.

Given that these compounds are bigger compared to L-kyn, we observed the reorientation of many of the hydrophobic residues as previously observed when UPF 648 was bound to the same enzyme[1]. This can be attributed to the fact that these compounds are much bigger compared to L-kyn and therefore result in the reorientation of some residues in order for them to fit in the active site and make essential contacts with active residues.

Conclusions

Our results validated our pharmacophore predictions that tertiary sulfonylureas inhibit both NOX and KMO. Though these compounds have a lot in common, the fluorination on the compounds had shown to have a great impact on the strength of the binding. This study opens a new therapeutic approach for neurodegenerative disorders by multi-targeting both KMO and NOX. The inhibition of KMO is known to not only decrease the production of neurotoxic KP metabolites but also shift the pathway to the production of a neuroprotectant, KA. We propose that inhibiting both KMO and NOX simultaneously will not only increase the neuroprotective effect of KA but also will maximize the OS reduction in the CNS. Further in vivo studies are needed to validate our hypothesis that inhibiting both NOX and KMO simultaneously using multi-targeting agents can potentially overcome current challenges in obtaining neurodegenerative drugs.

CHAPTER 5

FENBUFEN AND ITS PHENYL ALKANOIC ACID DERIVATIVES AS POTENT KYNURENINE MONOOXYGENASE INHIBITORS

Emma Carine Iradukunda, Grayson T. Beasley and Robert S. Phillips. To be submitted to *Medicinal Chemistry Research Journal*.

Abstract

Inhibition of kynurenine monooxygenase (KMO) is one of the current therapeutic targets of neurological and neurodegenerative disorders. Using our receptor-based pharmacophore as well as the structure-activity relationship we have been able to deduce, synthesize and validate six phenyl alkanoic acids as competitive inhibitors of *Cytophaga hutchinsonii* KMO. Our results indicate a nanomolar inhibitory potency of Fenbufen, a known FDA-approved nonsteroidal anti-inflammatory drug (NSAID). In addition to inhibiting KMO, Fenbufen does not uncouple nicotinamide adenine dinucleotide phosphate (NADPH) as it has been observed in some other KMO inhibitors. These findings validate our pharmacophore and establish phenyl alkaloids NSAIDs especially γ-oxobenzenebutanoic acids as viable lead compounds and eligible drug candidates for repurposing for neurodegenerative diseases.

Introduction

Notwithstanding advancements in biotechnology and pharmacology, there are still incurable diseases such as neurodegenerative disorders and most cancers. Discovering and developing a new drug is time-consuming and very costly [90]. In some cases, despite a lot of efforts to bring a new drug forward, thousands of FDA-approved drugs are removed from the market and recalled every year after they have reached pharmacies [91]. Therefore, repurposing FDA-approved drugs that were recalled or are still in use is an appreciated drug discovery route for coming up with new drugs. Given that drug candidates for repurposing/repositioning have already been thoroughly clinically tried and approved to be safe for humans, several steps for traditional drug discovery are omitted when studying them for new indications making the process time-efficient and cost-efficient[92-94].

Our lab is involved in researching suitable lead compounds for neurodegenerative disorders such as Alzheimer's (AD), Parkinson's (PD), and Huntington's (HD) diseases and several neurodegenerative disorders by targeting enzymes on the tryptophan pathway (TP) (Figure 5.1) such as kynurenine monooxygenase (KMO). KMO catalyzes the conversion of kynurenine (KYN) to a cytotoxic 3-hydroxykynurenine (3-HK) which eventually leads to a production of a neurotoxin quinolinic acid (QA). KYN is also a substrate of kynureninase and kynurenine aminotransferase (KAT) leading to the production of anthranilic acid (AA) and a neuroprotectant metabolite kynurenic acid (KA) respectively. Both QA and KA affect the regulation of glutamate receptors such as the N-methyl-D-aspartate receptor (NMDAr). KA antagonizes the NMDAr thereby acting as a neuroprotectant [33]. QA, on the other hand, is responsible for the loss of homeostasis of Ca^{2+} as it agonizes the NMDAr as it leads to an overload of Ca^{2+} which is detrimental to the mitochondria[22, 95, 96]. Researchers have shown

that KP is activated in events of neurodegeneration and major depressive disorders; thus, the increase in levels of QA and the decrease in KA levels is a biomarker to the above pathological disorders [41, 65, 69, 97]. Since KMO is at the branching point of KP, its inhibition is therefore thought to be an excellent therapeutic target.

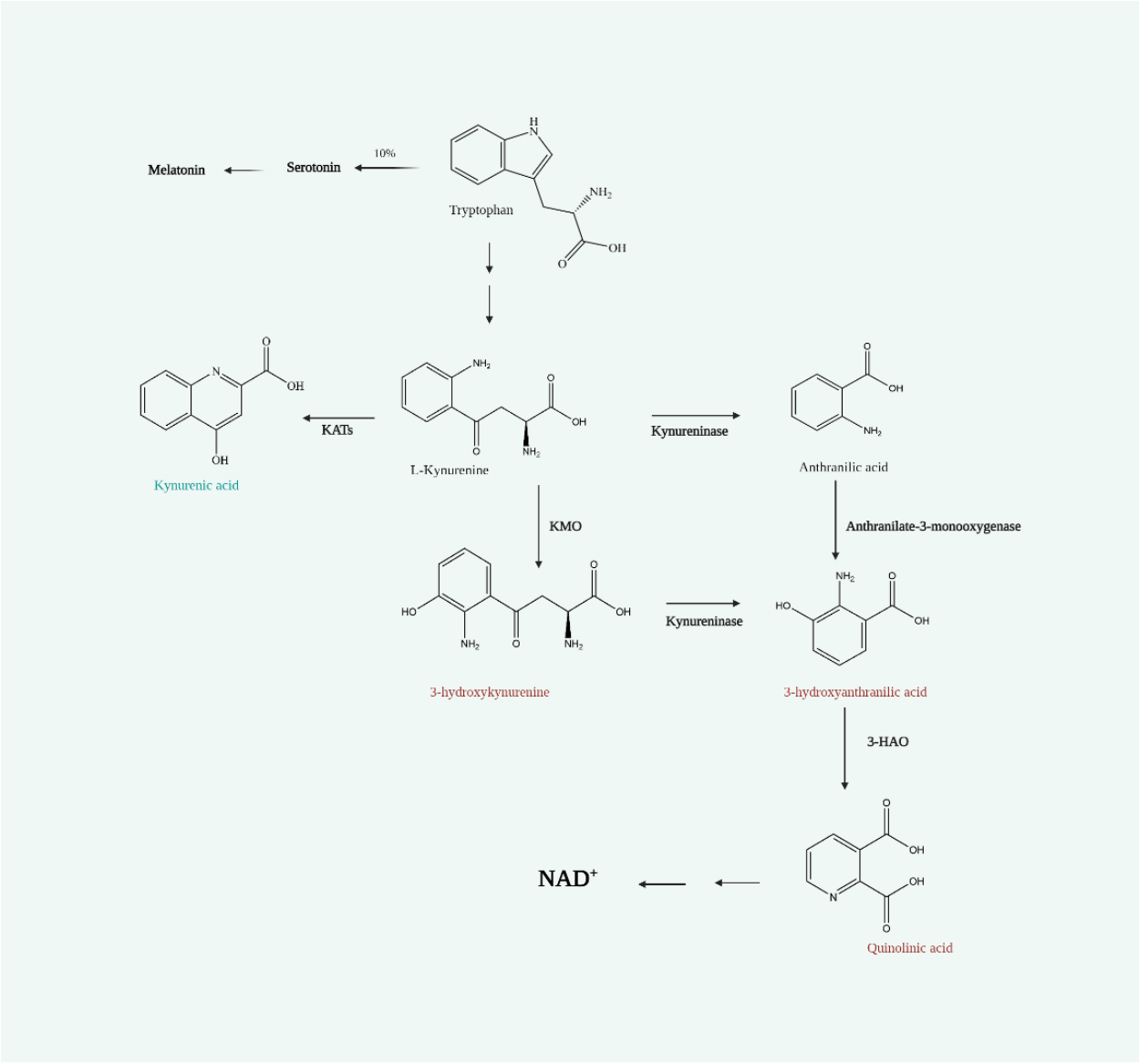

Figure 5.1. Kynurenine pathway highlighting neuroactive metabolites and relevance of KMO inhibition. Green: neuroprotective, red: neurotoxic.

Several lead compounds have been generated in the last two decades[51, 56, 57, 71, 98]mainly using structure-based and ligand-based drug design. Most recently a nonsteroidal anti-inflammatory (NSAID) drug, diclofenac, was proposed as a KMO binder/ inhibitor with a K_d in the lower micromolar range 13.6 μM[62]. Our recently designed pharmacophore model predicted several hits[56], among them, was PAA-1 (scheme 1) which is structurally similar to two FDA-approved phenyl alkanoic acid NSAIDS: bucloxic acid[99] (Figure 5.3) which was later recalled for unknown reasons, and fenbufen[100] which is still in use. We synthesized these compounds (Figure 5.2), then, using both kinetic and molecular modeling tools, we were able to provide further insights into how they bind to KMO and direct future considerations.

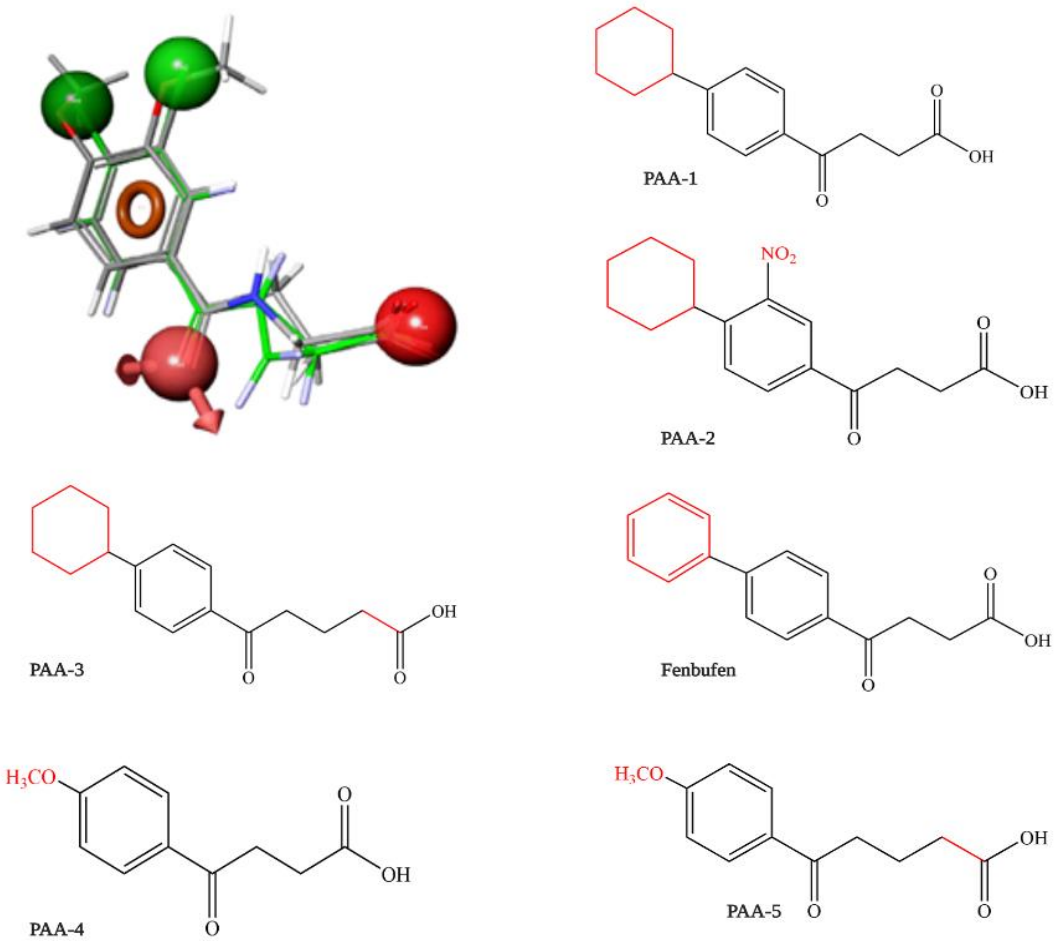

Figure 5.2. Structures of phenyl alkanoic acids that were evaluated in this study. PAA-1 was predicted by a pharmacophore model (top left) [56]. Using the structural similarities, we proposed PAA-2, PAA-3, PAA-4, PAA-5, and Fenbufen as potential KMO inhibitors.

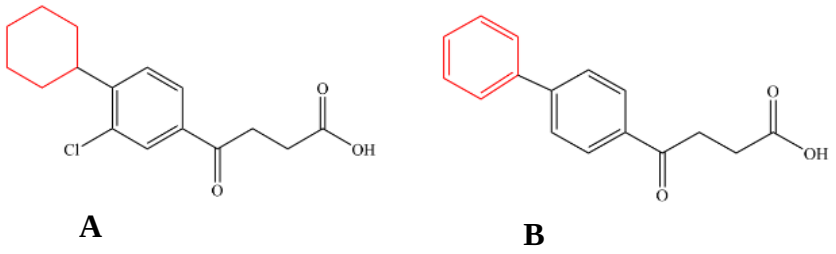

A **B**

Figure 5.3. FDA-approved NSAID Bucloxic acid (A) Fenbufen (B) on the right similar to our lead compound PAA-1.

Materials and Methods

Synthesis

The procedure for the Friedel-Crafts acylation used in this study was performed by Srinivas Et.al [101]and is briefly described here with slight modifications. Succinic anhydride and glutaric anhydride were recrystallized before their usage. 3.3 mmol of aluminum chloride, 3 mmol succinic anhydrides, and 5ml dichloromethane were added to a 200ml round bottom flask. The mixture was stirred and cooled to 15°C. The 3 mmol equivalence of the aromatic compound was added to the flask in a dropwise manner. The reaction was allowed to proceed for 24 hours under stirring conditions. After the completion of the reaction, the reaction mixture was added to a mixture of ice and concentrated HCl (10:1). The precipitate was suction filtered and washed with 2 rounds of 10ml of petroleum ether. HNMR was used to confirm the reaction was successful. Reaction yields were high (~90%) for all products excluding Fenbufen (<15%). Butanoic acid derivatives were synthesized with succinic anhydride; glutaric anhydride was used for pentanoic acid derivatives. The synthesis of Fenbufen required an additional acid-base workup step to isolate the final product. The precipitate was dissolved in 3M KOH. The mixture was suction filtered and washed with

deionized water. The filtrate was isolated and concentrated HCl was added to the precipitate product. The final product was isolated by suction filtration.

Purification of recombinant *cytophaga hutchinsonii* KMO

chKMO [72] was expressed *in E. coli* BL21 (DE3). A single colony grown on Luria broth (LB) /kanamycin agar plates, was removed and inoculated with an aliquot of 5 ml of sterile LB broth with 5µl kanamycin overnight at 37 °C with shaking at 180 rpm. That culture was then added to separate 2 L Erlenmeyer flasks containing 1 L Studier autoinduction medium[73]supplemented with 200mg/L kanamycin. The cells were then grown at 37°C for 24 hours with gentle agitation (220 rpm). After, the cells were collected by centrifugation for 15 minutes at 4000 rpm at 4 °C in 500 ml flasks using a Jouan CR422 centrifuge and stored at -80ºC until used for enzyme purification.

Cells were resuspended in 30 ml 0.05M Tris-acetate buffer supplemented with 1 mM DTT, 0.2% Triton X-100, and 5 µM FAD. The yellow suspension was sonicated on ice in 4 60-second bursts with 3 minutes cooling between bursts. Debris was removed by centrifugation for 1 hour 30 minutes at 4000 rpm at 4 °C in 60 mL tubes using a Sorvall RC 6 Plus centrifuge and a Sorvall SS-34 rotor. Additional purification was achieved by immobilized metal affinity and anion exchange chromatography using Ni-NTA column and DEAE columns, respectively.

Nickel column chromatography: The enzyme solution from the previous step was loaded on the Ni column equilibrated with 100ml 0.05 M Tris-acetate buffer (pH 8.0, 5 µM FAD, 0.5 mM DTT); then the protein was loaded, followed by washing with 100ml 0.005m Tris-acetate buffer (PH 8.0, 5 µM FAD, 0.5 mM DTT, 20mM imidazole) buffer. The protein was eluted overnight using 0.05 M Tris-acetate buffer (PH 8.0, 1 mM DTT, 200 mM imidazole).

The fractions that possessed a brilliant yellow color and contained significant KMO activity were pooled and concentrated using a centrifuge at 478080 x g at 4 C for 1 hour 3 times using the exchange buffer (0.05 M Tris-acetate buffer pH 8.0, 5 µM FAD, 0.5 mM DTT). *Diethylaminoethyl column (DEAE).* For further purification, the protein was loaded onto a DEAE column (30 cm · 2.5 cm) pre-equilibrated with 100ml of the same buffer used for Ni-NTA column buffer followed by washing with the same buffer with 20 mM NaCl instead of imidazole. The protein was eluted overnight using 100ml 0.05 M Tris-acetate buffer and 200 mM NaCl. The fractions that possessed a brilliant yellow color and contained significant KMO activity were pooled and concentrated using a centrifuge at 478080 x g at 4 C for 1 hour 3 times using the exchange buffer (0.05 M Tris-acetate buffer pH 8.0, 5 µM FAD, 0.5 mM DTT), this was then distributed into several Eppendorf tubes, flash-frozen with liquid nitrogen then stored at -80°C.

UV-Vis spectrophotometry for enzyme concentration

Protein determination. The concentration of purified chKMO was determined using a 1E UV-Vis spectrophotometer with a quartz cuvette of path length 1 cm. The concentration of chKMO was obtained by a scan between 400-200 nm for a solution of 10µL protein and 10µL 1M Kpi PH 7.0 in 380µL of water. The concentration was calculated using the Beer-Lambert law using the molar absorbance for flavin at 450 nm (12300 M-1 cm-1).

Steady-state observations /UV-VIS spectrophotometry

The enzyme activity was determined by monitoring the NADPH consumption by absorbance at 340 nm. The reaction mixture consisted of 530 µl of buffer (0.05 M Tris-acetate, pH 8.0, 1 mM DTT, 5 µM FAD), 6 µl 10 mM kynurenine, 10 µl 12 mM NADPH, 4 µl 1.5M KCl. The

reaction was initiated by the addition of 50 µl of enzyme sample (21.6 µM). Kinetic parameters were determined by initial velocity measurements at a fixed concentration of NADPH (0.5 mM) and varying concentrations of kynurenine. For the enzyme inhibition assays, the above procedure was applied with varying concentrations of the ligand. The inhibitor constant (Ki) values were obtained using Compo software[74].

Molecular modeling

Autodock vina with the PYMOL plugin was used to study the binding modes of our proposed compounds. We docked all our compounds to A PDB file (4j36) was obtained from a protein data bank. Before docking, we first prepared it by removing the ligand (UPF 648) using PyMol v1.4.1 followed by generating pdbqt file representing the protein. Our ligands were prepared using Chem3D 19.1, followed by generating PDBQT files representing them using PyMol v1.4.1. The following are the parameters we used in all our docking: Size (x=22; y=24; z=28), center (x=11; y=90.5; z=57.5).

Compound	**Ki/K_d (µM)**
PAA-1	0.846+/-0.1
PAA-2*	1.3+/-0.52
PAA-3	7.38+/-4.40
PAA-4	-
PAA-5	-
Fenbufen	0.38+/-0.14

Table 5.1. Binding affinities (K_D) of proposed phenyl alkanoic acids. Binding affinities were measured by the ligand perturbation of FAD fluorescence. PAA-2 could not be measured using the same method owing to the high noise because the attached nitro-group exhibits a fluorescence emission approximately the same as FAD. We have used the UV-vis spectrophotometer to measure the decrease in the NADPH absorbance at 340nm. PAA-4 and PAA-5 are weak binders, they could not saturate the enzyme, we expect their binding affinities to be in the millimolar range.

Discussion

In this study, we propose a library of NSAIDs and their derivatives as competitive inhibitors of chKMO. We used the receptor-based pharmacophore that was previously developed using a Schrödinger software package[88]. From this model, several kynurenine analogs were designed, synthesized, and tested as substrates, non-substrate effectors, and inhibitors of chKMO[56]. The kinetic assays used in this study were previously described elsewhere [1, 54, 72]but are mentioned here with slight modifications. We also used autodock vina with the PyMol plugin to predict the binding modes of our compounds as described in a similar recent study [62]. Because the purification of chKMO requires the use of detergent, it had been challenging to crystallize it[48, 102]. However, since the structure of scKMO is known and all residues that make contact with the substrate are conserved across the species, we have used scKMO (PDB code: 4J34) for docking purposes[1].

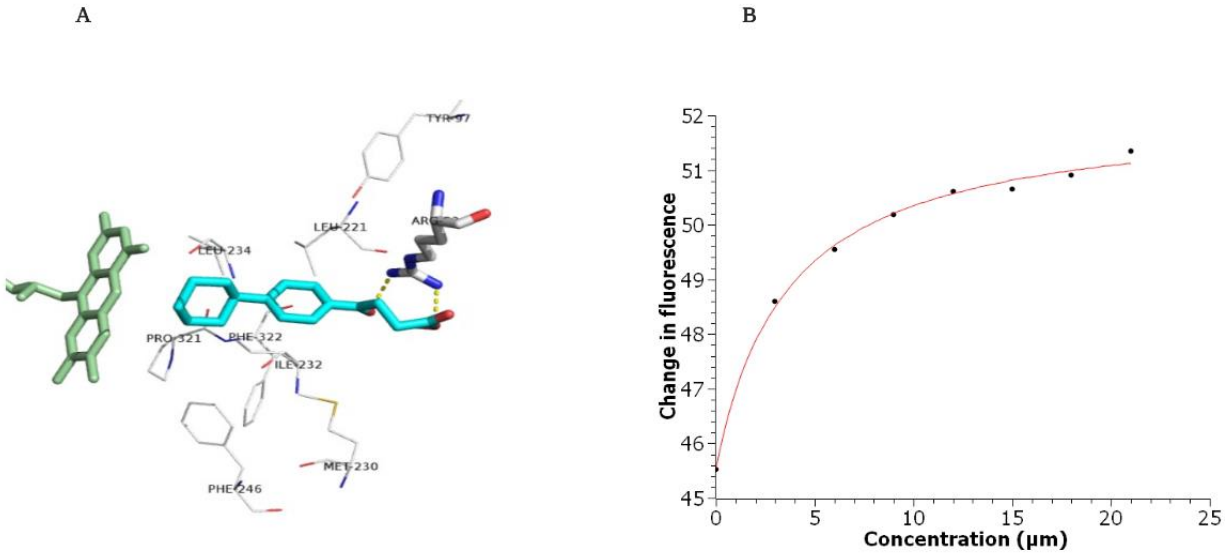

Figure 5.4. (A) active site of scKMO (PDB code: 4J34) in complex with PAA-1. **(B)** Binding affinity of PAA-1.

PAA-1 was the only compound in our library that was computationally predicted using this pharmacophore (Figure 5.2), the rest of the compounds were deduced using the structure-activity-relationship (SAR) approach and molecular similarity techniques. PAA-1 displayed an appreciable inhibitory potency with a K_d of 0.846+/-0.1µM (Figure 5.4). Its binding model resulted in a reorientation of TYR 97 making it have interactions only with ARG 83 via its carboxylate and carbonyl moieties. Both phenyl and aromatic rings occupied the hydrophobic pocket. The cyclohexyl ring adopted a chair conformation upon binding, giving it a lower energy binding. The tighter binding of PAA-1 can be attributed to the fact that the distance between the aromatic ring and the carboxylate moiety is the same as kynurenine, allowing it to exhibit an additional H-bonding between its carbonyl and the NH of the guanidino group of Arg83.

The first-ever proposed KMO inhibitor β-Benzoyl-L-alanine [54] was designed by removing the amino group on the benzene ring of L-kyn, further modification on the ring by adding a nitro group resulted in m-nitrobenzolyalalanine (m-NBA) which improved the binding and the inhibitory potency of the compound eight-fold [43]. The administration of m-NBA in mice had shown an improved regulation of NMDA receptor agonism and antagonism homeostasis in both the brain and blood. Also, there was an increased level of both L-kyn and KYNA to up 10 times and 5 times in the brain and blood, respectively, when about 400 mg/kg of m-NBA was administered in rats. Encouraged by this result we designed PAA-2 (Figure 5.2) by adding a nitro group on the benzene nucleus of PAA-1. The presence of an extra nitro group on the benzene rings did not affect the binding affinity as much as we expected. We observed a reorientation of active residues which created an extra interaction between the TYR 97 and carbonyl group on PAA-2 in addition to a strong hydrogen bond between Arg83 and carboxylate (Figure 5.5).

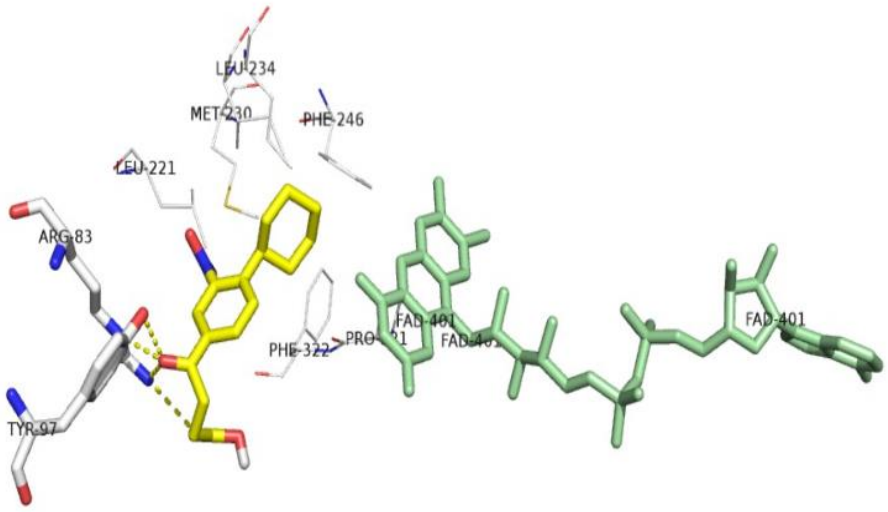

Figure 5.5. (A) the active site of scKMO (PDB code: 4J34) in complex with PAA-2.

Next, considering the structural similarities of PAA-1 to known FDA-approved phenyl alkanoic acid/ γ-oxobenzenebutanoic acids nonsteroidal anti-inflammatory (NSAID) drugs such as Fenbufen[103] we tested Fenbufen and its phenyl alkanoic acids derivatives (scheme 1) for KMO inhibition. Like NSAIDs in the phenyl alkanoic acid family, Fenbufen is a cyclooxygenase (COX) inhibitor that is primarily used to treat osteoarthritis, tendinitis, spondylitis, and ankylosing[104]. Their structural similarities led us to want to test Fenbufen as a potential inhibitor of KMO. We, therefore, synthesized Fenbufen and tested it for KMO inhibition. The binding was similar to that of PAA-1, though the aromatic ring sat in the hydrophobic region towards the re-side of FAD, the lack of flexibility of the benzene ring made it bind differently, making it have additional polar contact with Tyr 97 via the carboxylate (Figure 5.6).

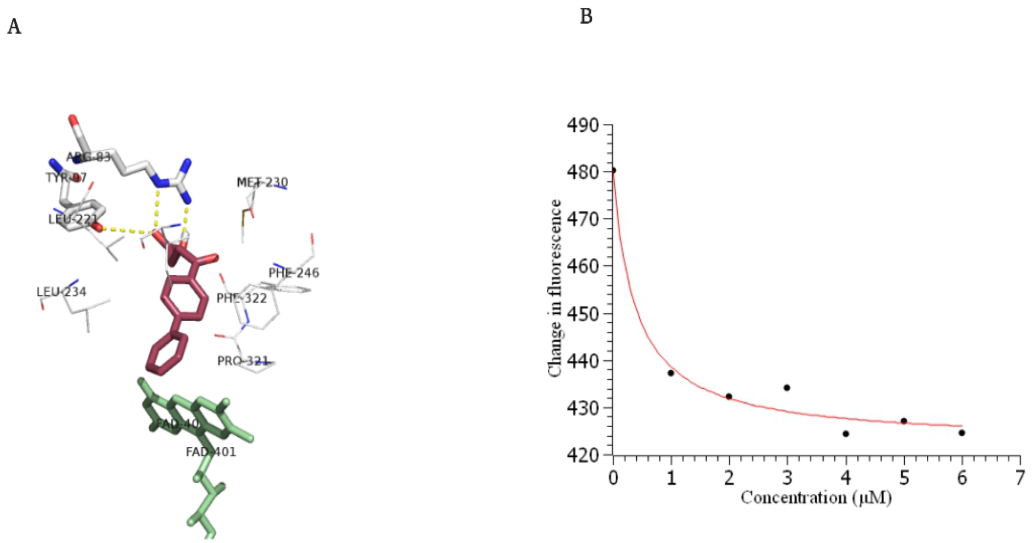

Figure 5.6. (**A)** The active site of scKMO (PDB code: 4J34) in complex with Fenbufen. **(B)** Binding affinity of Fenbufen.

Our original pharmacophore was designed after recognizing that there needed to be 3 spacers between the aromatic ring and the carboxylic acid centers. To determine the necessity of three carbon spacers atoms between the benzene ring and carboxylate moiety in inhibitory potency, we synthesized PAA-3 with an additional carbon. Though the arginine-carboxylate interaction was maintained (Figure 5.7), the presence of an extra carbon reduced the binding affinity eight-fold (Table 5.1).

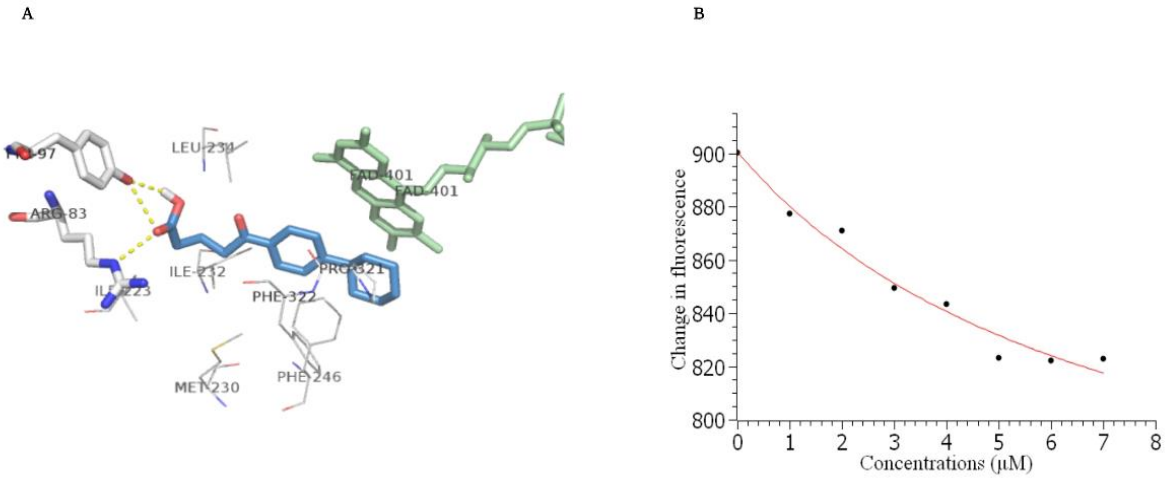

Figure 5.7: (A) active site of scKMO (PDB code: 4J34) in complex with PAA-3. **(B)** Binding affinity of PAA-3.

We also assessed the effect of changing the polarity of these compounds by replacing the cyclohexyl with methoxy in PAA-4 and PAA-5. The methoxy made an additional hydrogen bond with a water molecule and the carbonyl group of the isoalloxazine ring system of FAD.

Despite that the polar contacts with both Arg83 and Tyr 97 via its carboxylic acid moiety (see Figure 5.8), the inhibition potency was greatly affected. This poor binding highlights the importance of hydrophobicity on the left side of the ring for a better binding.

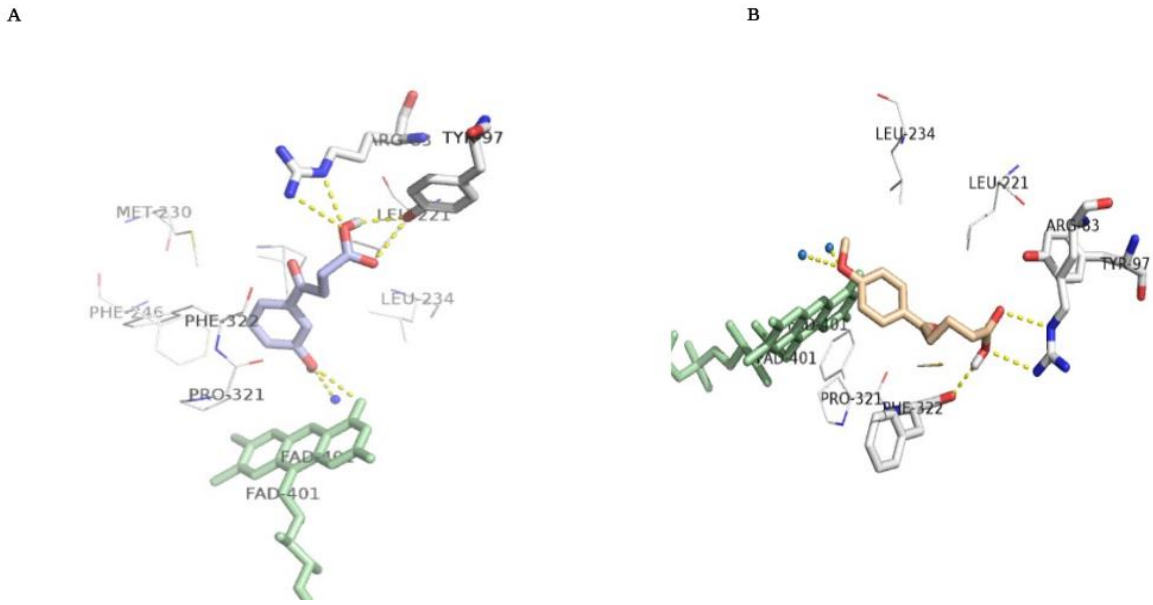

Figure 5.8. The structure of scKMO (pdb:4J) bound to FAD and PAA-4 **(A)** and PAA-5 **(B).**

Conclusions

Our receptor-based pharmacophore predicted PAA-1 as a potential competitive inhibitor of chKMO. Using SAR and molecular similarity techniques, we have further demonstrated that both PAA-1 and Fenbufen competitively inhibit chKMO in the nanomolar range. Our results together with a recent study [62] on Diclofenac show that indeed, phenyl alkanoic acids NSAIDS make good KMO inhibitors provided that they share core structure similarities with known KMO inhibitors especially kynurenine analogs. It is not unusual that one compound

can target multiple enzymes/receptors provided that it meets all binding requirements for both enzymes. Drug repurposing remains the most attractive drug discovery route in bringing forth treatments for new indications from FDA-approved drugs both recalled and still in use [90, 92]. It is even more appreciated in dealing with incurable diseases or pandemic diseases that need immediate attention.

CHAPTER 6

CONCLUSIONS

Despite the rise in numbers of people who suffer from different neurodegenerative diseases globally, treatment remains unknown owing to the multifactorial nature of these diseases and sometimes the irreversibility of neuron damage. There are several enzymes targeted for finding a cure, and this work focused on KMO on the kynurenine pathway. To date, the purification and crystallization of a full-length active hKMO have been unsuccessful and as a result, research on KMO has been performed using the enzyme from other species such as pf, sc, and ch. Most previous works were performed on *Pseudomonas fluorescens* and *Saccharomyces cerevisiae* of which purification is very well established. The present work was performed on *Cytophaga hutchinsonii (chKMO),* we proposed a new protocol of purification of this species, however, given that chKMO is a membrane-associated enzyme, detergent (triton) was used in the purification process which resulted in unsuccessful crystallization attempts. Nonetheless, since all residues that make contact with the substrate are conserved in other species, we have docked our compounds using the scKMO model for us to learn their binding modes. In this study, we have also proposed several lead compounds as chKMO binders. We have shown how compounds that bind to other enzymes such as COX, NOX4, and KYNU can bind to chKMO as well, opening doors to the possibility of repurposing some already FDA-approved drugs as well as multi-targeting several enzymes that have implications in neurodegeneration without having to use combination therapy.

Despite the good binding of some KMO binders, several have previously shown that they only inhibit the product formation, meaning that they prevent the substrate from being hydroxylated, but they still uncouple NADPH which leads to an eventual accumulation of hydrogen peroxides. We have observed this phenomenon in 5-NKyn which is structurally similar to an already known and well-studied KMO binder mNBA. Though previous studies already suggested that kynurenine analogs with substitution on C-5 are good substrates, the lack of hydroxylation on 5-NKyn suggests that the presence of a strong deactivating group such as nitro is responsible for the lack of reactivity of this compound. Therefore, though we show that this compound binds to KMO and inhibits the hydroxylation of kynurenine further structural modifications are needed to present this side effect.

The accumulation of ROS in the CNS is responsible for the initiation and progression of neurodegeneration by causing neuron damage. We have shown that SAPCO, an already known KYNU also inhibits KMO, and these two enzymes are known to lead to the production of free radical generators. Since the inhibition of KMO only requires a carboxylic acid moiety for binding and KYNU requires the amino group, we hypothesize that kynurenine analogs with both an amino group and carboxylic acid moieties would make good multitargeting candidates for both KYNU and KMO. In vivo studies would help determine if SAPCO simultaneously inhibits these two enzymes.

Additionally, two pharmacophore models were previously designed, one for KMO and another for NOX inhibitors. They have predicted tertiary sulfonylureas as potential inhibitors for these enzymes. Our results validated our pharmacophore predictions that tertiary sulfonylureas inhibit both NOX and KMO. We noticed that fluorination of the compounds has a great impact on the strength of the binding. This study opens a new therapeutic approach for neurodegenerative

disorders by multi-targeting both KMO and NOX. The inhibition of KMO is known to not only decrease the production of neurotoxic KP metabolites but also shift the pathway to the production of a neuroprotectant, KA. We propose that inhibiting both KMO and NOX simultaneously will not only increase the neuroprotective effect of KA but also will maximize the OS reduction in the CNS. Further in vivo studies are needed to validate our hypothesis that inhibiting both NOX and KMO simultaneously using multi-targeting agents can potentially overcome current challenges in obtaining neurodegenerative drugs.

Last, but certainly not least, are phenylalkanoic acid NSAIDS and their derivatives. Again, using the same pharmacophore that predicted our sulfonylureas, PAA-1 was initially predicted to inhibit KMO. However, the structural similarities of these compounds to commercially available and FDA-approved NSAIDs lead us to propose Fenbufen and other derivatives for KMO inhibition. And indeed, the results were very encouraging. There is a lot of advantages to this finding, given that these compounds already have FDA approval making these compounds the best lead candidates in our library.

REFERENCES

1. Amaral, M.; Levy, C.; Heyes, D. J.; Lafite, P.; Outeiro, T. F.; Giorgini, F.; Leys, D.; Scrutton, N. S., Structural basis of kynurenine 3-monooxygenase inhibition. *Nature* **2013,** *496* (7445), 382-385.

2. center, H. N., The Challenge of Neurodegenerative Diseases.

3. Swinney, D. C.; Anthony, J., How were new medicines discovered? *Nature Reviews Drug Discovery* **2011,** *10* (7), 507-519.

4. Muto, A.; Orger, M. B.; Wehman, A. M.; Smear, M. C.; Kay, J. N.; Page-McCaw, P. S.; Gahtan, E.; Xiao, T.; Nevin, L. M.; Gosse, N. J.; Staub, W.; Finger-Baier, K.; Baier, H., Forward Genetic Analysis of Visual Behavior in Zebrafish. *PLOS Genetics* **2005,** *1* (5), e66.

5. Ecker, A.; Bushell, E. S.; Tewari, R.; Sinden, R. E., Reverse genetics screen identifies six proteins important for malaria development in the mosquito. *Mol Microbiol* **2008,** *70* (1), 209-20.

6. Pardo, L. M.; van Duijn, C. M., In search of genes involved in neurodegenerative disorders. *Mutat Res* **2005,** *592* (1-2), 89-101.

7. Bolognesi, M. L., Polypharmacology in a single drug: multitarget drugs. *Curr Med Chem* **2013,** *20* (13), 1639-45.

8. de Lera, A. R.; Ganesan, A., Epigenetic polypharmacology: from combination therapy to multitargeted drugs. *Clinical Epigenetics* **2016,** *8* (1), 105.

9. Bolognesi, M. L.; Cavalli, A., Multitarget Drug Discovery and Polypharmacology. *ChemMedChem* **2016,** *11* (12), 1190-2.

10. Zhou, Q.; Sheng, M., NMDA receptors in nervous system diseases. *Neuropharmacology* **2013,** *74*, 69-75.

11. Liu, J.; Chang, L.; Song, Y.; Li, H.; Wu, Y., The Role of NMDA Receptors in Alzheimer's Disease. *Frontiers in Neuroscience* **2019,** *13* (43).

12. Zamponi, G. W., Targeting voltage-gated calcium channels in neurological and psychiatric diseases. *Nature Reviews Drug Discovery* **2016,** *15* (1), 19-34.

13. Heyes, S.; Pratt, W. S.; Rees, E.; Dahimene, S.; Ferron, L.; Owen, M. J.; Dolphin, A. C., Genetic disruption of voltage-gated calcium channels in psychiatric and neurological disorders. *Prog Neurobiol* **2015,** *134*, 36-54.

14. Dawson, V. L.; Dawson, T. M., Nitric oxide in neurodegeneration. *Prog Brain Res* **1998,** *118*, 215-29.

15. Barua, S.; Kim, J. Y.; Yenari, M. A.; Lee, J. E., The role of NOX inhibitors in neurodegenerative diseases. *IBRO reports* **2019,** *7*, 59-69.

16. Niedzielska, E.; Smaga, I.; Gawlik, M.; Moniczewski, A.; Stankowicz, P.; Pera, J.; Filip, M., Oxidative Stress in Neurodegenerative Diseases. *Molecular Neurobiology* **2016,** *53* (6), 4094-4125.

17. Ross, C. A.; Poirier, M. A., Protein aggregation and neurodegenerative disease. *Nat Med* **2004,** *10 Suppl*, S10-7.

18. Soto, C.; Pritzkow, S., Protein misfolding, aggregation, and conformational strains in neurodegenerative diseases. *Nature Neuroscience* **2018,** *21* (10), 1332-1340.

19. Vaquer-Alicea, J.; Diamond, M. I., Propagation of Protein Aggregation in Neurodegenerative Diseases. *Annual Review of Biochemistry* **2019,** *88* (1), 785-810.

20. Young, W., Role of calcium in central nervous system injuries. *J Neurotrauma* **1992,** *9 Suppl 1*, S9-25.

21. Marambaud, P.; Dreses-Werringloer, U.; Vingtdeux, V., Calcium signaling in neurodegeneration. *Molecular Neurodegeneration* **2009,** *4* (1), 20.

22. Lin, M. T.; Beal, M. F., Mitochondrial dysfunction and oxidative stress in neurodegenerative diseases. *Nature* **2006,** *443* (7113), 787-795.

23. Wagner, B. A.; Venkataraman, S.; Buettner, G. R., The rate of oxygen utilization by cells. *Free Radic Biol Med* **2011,** *51* (3), 700-12.

24. Sayre, L. M.; Perry, G.; Smith, M. A., Oxidative stress and neurotoxicity. *Chem Res Toxicol* **2008,** *21* (1), 172-88.

25. Wang, X.; Wang, W.; Li, L.; Perry, G.; Lee, H. G.; Zhu, X., Oxidative stress and mitochondrial dysfunction in Alzheimer's disease. *Biochim Biophys Acta* **2014,** *1842* (8), 1240-7.

26. Peters, J. C., Tryptophan nutrition and metabolism: an overview. *Adv Exp Med Biol* **1991,** *294*, 345-58.

27. Kang, K.; Lee, K.; Park, S.; Kim, Y. S.; Back, K., Enhanced production of melatonin by ectopic overexpression of human serotonin N-acetyltransferase plays a role in cold resistance in transgenic rice seedlings. *J Pineal Res* **2010,** *49* (2), 176-82.

28. Stone, T. W., Neuropharmacology of quinolinic and kynurenic acids. *Pharmacol Rev* **1993,** *45* (3), 309-79.

29. Rios, C.; Santamaria, A., Quinolinic acid is a potent lipid peroxidant in rat brain homogenates. *Neurochemical Research* **1991,** *16* (10), 1139-1143.

30. Santamaría, A.; Jiménez-Capdeville, M. E.; Camacho, A.; Rodríguez-Martínez, E.; Flores, A.; Galván-Arzate, S., In vivo hydroxyl radical formation after quinolinic acid infusion into rat corpus striatum. *Neuroreport* **2001,** *12* (12), 2693-2696.

31. Santamaría, A.; Galván-Arzate, S.; Lisý, V.; Ali, S. F.; Duhart, H. M.; Osorio-Rico, L.; Ríos, C.; St'astný, F., Quinolinic acid induces oxidative stress in rat brain synaptosomes. *Neuroreport* **2001,** *12* (4), 871-874.

32. Behan, W. M.; McDonald, M.; Darlington, L. G.; Stone, T. W., Oxidative stress as a mechanism for quinolinic acid-induced hippocampal damage: protection by melatonin and deprenyl. *British journal of pharmacology* **1999,** *128* (8), 1754-1760.

33. Winn, P.; Stone, T. W.; Latimer, M.; Hastings, M. H.; Clark, A. J., A comparison of excitotoxic lesions of the basal forebrain by kainate, quinolinate, ibotenate, N-methyl-D-aspartate or quisqualate, and the effects on toxicity of 2-amino-5-phosphonovaleric acid and kynurenic acid in the rat. *British journal of pharmacology* **1991,** *102* (4), 904-908.

34. Foster, A. C.; Vezzani, A.; French, E. D.; Schwarcz, R., Kynurenic acid blocks neurotoxicity and seizures induced in rats by the related brain metabolite quinolinic acid. *Neurosci Lett* **1984,** *48* (3), 273-8.

35. Heyes, M. P., Metabolism and neuropathologic significance of quinolinic acid and kynurenic acid. *Biochemical Society Transactions* **1993,** *21* (1), 83-89.

36. Mole, D. J.; Webster, S. P.; Uings, I.; Zheng, X.; Binnie, M.; Wilson, K.; Hutchinson, J. P.; Mirguet, O.; Walker, A.; Beaufils, B.; Ancellin, N.; Trottet, L.; Bénéton, V.; Mowat, C. G.; Wilkinson, M.; Rowland, P.; Haslam, C.; McBride, A.; Homer, N. Z.; Baily, J. E.; Sharp, M. G.; Garden, O. J.; Hughes, J.; Howie, S. E.; Holmes, D. S.; Liddle, J.; Iredale, J. P.,

Kynurenine-3-monooxygenase inhibition prevents multiple organ failure in rodent models of acute pancreatitis. *Nat Med* **2016,** *22* (2), 202-9.

37. Réus, G. Z.; Jansen, K.; Titus, S.; Carvalho, A. F.; Gabbay, V.; Quevedo, J., Kynurenine pathway dysfunction in the pathophysiology and treatment of depression: Evidences from animal and human studies. *Journal of Psychiatric Research* **2015,** *68*, 316-328.

38. Erhardt, S.; Schwieler, L.; Imbeault, S.; Engberg, G., The kynurenine pathway in schizophrenia and bipolar disorder. *Neuropharmacology* **2017,** *112* (Pt B), 297-306.

39. Giil, L. M.; Midttun, Ø.; Refsum, H.; Ulvik, A.; Advani, R.; Smith, A. D.; Ueland, P. M., Kynurenine Pathway Metabolites in Alzheimer's Disease. *Journal of Alzheimer's Disease* **2017,** *60*, 495-504.

40. Beal, M. F.; Kowall, N. W.; Ellison, D. W.; Mazurek, M. F.; Swartz, K. J.; Martin, J. B., Replication of the neurochemical characteristics of Huntington's disease by quinolinic acid. *Nature* **1986,** *321* (6066), 168-71.

41. Lim, C. K.; Fernández-Gomez, F. J.; Braidy, N.; Estrada, C.; Costa, C.; Costa, S.; Bessede, A.; Fernandez-Villalba, E.; Zinger, A.; Herrero, M. T.; Guillemin, G. J., Involvement of the kynurenine pathway in the pathogenesis of Parkinson's disease. *Progress in Neurobiology* **2017,** *155*, 76-95.

42. Schwarcz, R.; Bruno, J. P.; Muchowski, P. J.; Wu, H.-Q., Kynurenines in the mammalian brain: when physiology meets pathology. *Nature Reviews Neuroscience* **2012,** *13* (7), 465-477.

43. Chiarugi, A.; Carpenedo, R.; Moroni, F., Kynurenine Disposition in Blood and Brain of Mice: Effects of Selective Inhibitors of Kynurenine Hydroxylase and of Kynureninase. *Journal of Neurochemistry* **1996,** *67* (2), 692-698.

44. Erickson, J. B.; Flanagan, E. M.; Russo, S.; Reinhard, J. F., Jr., A radiometric assay for kynurenine 3-hydroxylase based on the release of 3H2O during hydroxylation of L-[3,5-3H]kynurenine. *Anal Biochem* **1992,** *205* (2), 257-62.

45. Guillemin, G. J.; Smith, D. G.; Smythe, G. A.; Armati, P. J.; Brew, G. J., Expression of The Kynurenine Pathway Enzymes in Human Microglia and Macrophages. In *Developments in Tryptophan and Serotonin Metabolism*, Allegri, G.; Costa, C. V. L.; Ragazzi, E.; Steinhart, H.; Varesio, L., Eds. Springer US: Boston, MA, 2003; pp 105-112.

46. Okamoto, H.; Yamamoto, S.; Nozaki, M.; Hayaishi, O., On the submitochondrial localization of l-kynurenine-3-hydroxylase. *Biochem Biophys Res Commun* **1967,** *26* (3), 309-14.

47. Alberati-Giani, D.; Cesura, A. M.; Broger, C.; Warren, W. D.; Röver, S.; Malherbe, P., Cloning and functional expression of human kynurenine 3-monooxygenase. *FEBS Letters* **1997,** *410* (2), 407-412.

48. Breton, J.; Avanzi, N.; Magagnin, S.; Covini, N.; Magistrelli, G.; Cozzi, L.; Isacchi, A., Functional characterization and mechanism of action of recombinant human kynurenine 3-hydroxylase. *European Journal of Biochemistry* **2000,** *267* (4), 1092-1099.

49. Garavito, R. M.; Picot, D.; Loll, P. J., Strategies for crystallizing membrane proteins. *J Bioenerg Biomembr* **1996,** *28* (1), 13-27.

50. Gao, J.; Yao, L.; Xia, T.; Liao, X.; Zhu, D.; Xiang, Y., Biochemistry and structural studies of kynurenine 3-monooxygenase reveal allosteric inhibition by Ro 61-8048. *Faseb j* **2018,** *32* (4), 2036-2045.

51. Hutchinson, J. P.; Rowland, P.; Taylor, M. R. D.; Christodoulou, E. M.; Haslam, C.; Hobbs, C. I.; Holmes, D. S.; Homes, P.; Liddle, J.; Mole, D. J.; Uings, I.; Walker, A. L.; Webster, S. P.; Mowat, C. G.; Chung, C.-w., Structural and mechanistic basis of differentiated

inhibitors of the acute pancreatitis target kynurenine-3-monooxygenase. *Nature Communications* **2017,** *8* (1), 15827.

52. Colabroy, K. L.; Begley, T. P., The pyridine ring of NAD is formed by a nonenzymatic pericyclic reaction. *J Am Chem Soc* **2005,** *127* (3), 840-1.

53. Altschul, S. F.; Gish, W.; Miller, W.; Myers, E. W.; Lipman, D. J., Basic local alignment search tool. *J Mol Biol* **1990,** *215* (3), 403-10.

54. Crozier-Reabe, K. R.; Phillips, R. S.; Moran, G. R., Kynurenine 3-Monooxygenase from *Pseudomonas fluorescens*: Substrate-like Inhibitors both Stimulate Flavin Reduction and Stabilize the Flavin−Peroxo Intermediate yet Result in the Production of Hydrogen Peroxide. *Biochemistry* **2008,** *47* (47), 12420-12433.

55. Speciale, C.; Wu, H. Q.; Cini, M.; Marconi, M.; Varasi, M.; Schwarcz, R., (R,S)-3,4-dichlorobenzoylalanine (FCE 28833A) causes a large and persistent increase in brain kynurenic acid levels in rats. *Eur J Pharmacol* **1996,** *315* (3), 263-7.

56. Phillips, R. S.; Anderson, A. D.; Gentry, H. G.; Güner, O. F.; Bowen, J. P., Substrate and inhibitor specificity of kynurenine monooxygenase from *Cytophaga hutchinsonii*. *Bioorganic & Medicinal Chemistry Letters* **2017,** *27* (8), 1705-1708.

57. Röver, S.; Cesura, A. M.; Huguenin, P.; Kettler, R.; Szente, A., Synthesis and biochemical evaluation of N-(4-phenylthiazol-2-yl)benzenesulfonamides as high-affinity inhibitors of kynurenine 3-hydroxylase. *J Med Chem* **1997,** *40* (26), 4378-85.

58. Zwilling, D.; Huang, S.-Y.; Sathyasaikumar, K. V.; Notarangelo, F. M.; Guidetti, P.; Wu, H.-Q.; Lee, J.; Truong, J.; Andrews-Zwilling, Y.; Hsieh, E. W.; Louie, J. Y.; Wu, T.; Scearce-Levie, K.; Patrick, C.; Adame, A.; Giorgini, F.; Moussaoui, S.; Laue, G.; Rassoulpour, A.; Flik, G.; Huang, Y.; Muchowski, J. M.; Masliah, E.; Schwarcz, R.;

Muchowski, P. J., Kynurenine 3-monooxygenase inhibition in blood ameliorates neurodegeneration. *Cell* **2011,** *145* (6), 863-874.

59. Giordani, A.; Pevarello, P.; Cini, M.; Bormetti, R.; Greco, F.; Toma, S.; Speciale, C.; Varasi, M., 4-Phenyl-4-oxo-butanoic acid derivatives inhibitors of kynurenine 3-hydroxylase. *Bioorg Med Chem Lett* **1998,** *8* (20), 2907-12.

60. Toledo-Sherman, L. M.; Prime, M. E.; Mrzljak, L.; Beconi, M. G.; Beresford, A.; Brookfield, F. A.; Brown, C. J.; Cardaun, I.; Courtney, S. M.; Dijkman, U.; Hamelin-Flegg, E.; Johnson, P. D.; Kempf, V.; Lyons, K.; Matthews, K.; Mitchell, W. L.; O'Connell, C.; Pena, P.; Powell, K.; Rassoulpour, A.; Reed, L.; Reindl, W.; Selvaratnam, S.; Friley, W. W.; Weddell, D. A.; Went, N. E.; Wheelan, P.; Winkler, C.; Winkler, D.; Wityak, J.; Yarnold, C. J.; Yates, D.; Munoz-Sanjuan, I.; Dominguez, C., Development of a Series of Aryl Pyrimidine Kynurenine Monooxygenase Inhibitors as Potential Therapeutic Agents for the Treatment of Huntington's Disease. *Journal of Medicinal Chemistry* **2015,** *58* (3), 1159-1183.

61. Lowe, D. M.; Gee, M.; Haslam, C.; Leavens, B.; Christodoulou, E.; Hissey, P.; Hardwicke, P.; Argyrou, A.; Webster, S. P.; Mole, D. J.; Wilson, K.; Binnie, M.; Yard, B. A.; Dean, T.; Liddle, J.; Uings, I.; Hutchinson, J. P., Lead Discovery for Human Kynurenine 3-Monooxygenase by High-Throughput RapidFire Mass Spectrometry. *Journal of Biomolecular Screening* **2013,** *19* (4), 508-515.

62. Shave, S.; McGuire, K.; Pham, N. T.; Mole, D. J.; Webster, S. P.; Auer, M., Diclofenac Identified as a Kynurenine 3-Monooxygenase Binder and Inhibitor by Molecular Similarity Techniques. *ACS Omega* **2018,** *3* (3), 2564-2568.

63. Kim, H. T.; Na, B. K.; Chung, J.; Kim, S.; Kwon, S. K.; Cha, H.; Son, J.; Cho, J. M.; Hwang, K. Y., Structural Basis for Inhibitor-Induced Hydrogen Peroxide Production by Kynurenine 3-Monooxygenase. *Cell Chemical Biology* **2018,** *25* (4), 426-438.e4.

64. Moroni, F.; Cozzi, A.; Peruginelli, F.; Carpenedo, R.; Pellegrini-Giampietro, D. E., Neuroprotective effects of kynurenine-3-hydroxylase inhibitors in models of brain ischemia. *Adv Exp Med Biol* **1999,** *467*, 199-206.

65. Heyes, M. P.; Saito, K.; Crowley, J. S.; Davis, L. E.; Demitrack, M. A.; Der, M.; Dilling, L. A.; Elia, J.; Kruesi, M. J.; Lackner, A.; et al., Quinolinic acid and kynurenine pathway metabolism in inflammatory and non-inflammatory neurological disease. *Brain* **1992,** *115 (Pt 5)*, 1249-73.

66. Dong-Ruyl, L.; Sawada, M.; Nakano, K., Tryptophan and its metabolite, kynurenine, stimulate expression of nerve growth factor in cultured mouse astroglial cells. *Neurosci Lett* **1998,** *244* (1), 17-20.

67. Nakagami, Y.; Saito, H.; Katsuki, H., 3-Hydroxykynurenine toxicity on the rat striatum in vivo. *Japanese journal of pharmacology* **1996,** *71* (2), 183-186.

68. Boegman, R. J.; Jhamandas, K.; Beninger, R. J., Neurotoxicity of Tryptophan Metabolitesa. *Annals of the New York Academy of Sciences* **1990,** *585* (1), 261-273.

69. Guillemin, G. J.; Brew, B. J., Implications of the kynurenine pathway and quinolinic acid in Alzheimer's disease. *Redox Rep* **2002,** *7* (4), 199-206.

70. Boegman, R. J.; El-Defrawy, S. R.; Jhamandas, K.; Beninger, R. J.; Ludwin, S. K., Quinolinic acid neurotoxicity in the nucleus basalis antagonized by kynurenic acid. *Neurobiology of Aging* **1985,** *6* (4), 331-336.

71. Natalini, B.; Mattoli, L.; Pellicciari, R.; Carpenedo, R.; Chiarugi, A.; Moroni, F., Synthesis and activity of enantiopure (S) (m-nitrobenzoyl) alanine, potent kynurenine-3-hydroxylase inhibitor. *Bioorganic & Medicinal Chemistry Letters* **1995,** *5* (14), 1451-1454.

72. Kurnasov, O.; Goral, V.; Colabroy, K.; Gerdes, S.; Anantha, S.; Osterman, A.; Begley, T. P., NAD Biosynthesis: Identification of the Tryptophan to Quinolinate Pathway in Bacteria. *Chemistry & Biology* **2003,** *10* (12), 1195-1204.

73. Studier, F. W., Protein production by auto-induction in high density shaking cultures. *Protein Expr Purif* **2005,** *41* (1), 207-34.

74. Wallace Cleland, W., [6] Statistical analysis of enzyme kinetic data. In *Methods in Enzymology*, Academic Press: 1979; Vol. 63, pp 103-138.

75. Ramsay, R. R.; Popovic-Nikolic, M. R.; Nikolic, K.; Uliassi, E.; Bolognesi, M. L., A perspective on multi-target drug discovery and design for complex diseases. *Clinical and translational medicine* **2018,** *7* (1), 3-3.

76. Floyd, R. A., Neuroinflammatory processes are important in neurodegenerative diseases: an hypothesis to explain the increased formation of reactive oxygen and nitrogen species as major factors involved in neurodegenerative disease development. *Free Radic Biol Med* **1999,** *26* (9-10), 1346-55.

77. Calabrese, V.; Bates, T. E.; Stella, A. M., NO synthase and NO-dependent signal pathways in brain aging and neurodegenerative disorders: the role of oxidant/antioxidant balance. *Neurochem Res* **2000,** *25* (9-10), 1315-41.

78. Sayre, L. M.; Moreira, P. I.; Smith, M. A.; Perry, G., Metal ions and oxidative protein modification in neurological disease. *Ann Ist Super Sanita* **2005,** *41* (2), 143-64.

79. Donnelly, P. S.; Xiao, Z.; Wedd, A. G., Copper and Alzheimer's disease. *Curr Opin Chem Biol* **2007,** *11* (2), 128-33.

80. Kim, D.-K.; Song, J.-W.; Park, J.-D.; Choi, B.-S., Copper induces the accumulation of amyloid-beta in the brain. *Molecular & Cellular Toxicology* **2013,** *9* (1), 57-66.

81. Saito, K.; Markey, S. P.; Heyes, M. P., Effects of immune activation on quinolinic acid and neuroactive kynurenines in the mouse. *Neuroscience* **1992,** *51* (1), 25-39.

82. Cozzi, A.; Carpenedo, R.; Moroni, F., Kynurenine Hydroxylase Inhibitors Reduce Ischemic Brain Damage: Studies with (m-Nitrobenzoyl)-Alanine (mNBA) and 3,4-Dimethoxy-[-N-4-(Nitrophenyl)Thiazol-2YL]-Benzenesulfonamide (Ro 61-8048) in Models of Focal or Global Brain Ischemia. *Journal of Cerebral Blood Flow & Metabolism* **1999,** *19* (7), 771-777.

83. Nagel, S.; Hadley, G.; Pfleger, K.; Grond-Ginsbach, C.; Buchan, A. M.; Wagner, S.; Papadakis, M., Suppression of the inflammatory response by diphenyleneiodonium after transient focal cerebral ischemia. *Journal of Neurochemistry* **2012,** *123* (s2), 98-107.

84. He, Y.-f.; Chen, H.-j.; Qian, L.-h.; He, L.-f.; Buzby, J. S., Diphenyleneiodonium protects preoligodendrocytes against endotoxin-activated microglial NADPH oxidase-generated peroxynitrite in a neonatal rat model of periventricular leukomalacia. *Brain Research* **2013,** *1492,* 108-121.

85. Wang, Q.; Qian, L.; Chen, S.-H.; Chu, C.-H.; Wilson, B.; Oyarzabal, E.; Ali, S.; Robinson, B.; Rao, D.; Hong, J.-S., Post-treatment with an ultra-low dose of NADPH oxidase inhibitor diphenyleneiodonium attenuates disease progression in multiple Parkinson's disease models. *Brain* **2015,** *138* (5), 1247-1262.

86. Xu, Q.; Kulkarni, A. A.; Sajith, A. M.; Hussein, D.; Brown, D.; Güner, O. F.; Reddy, M. D.; Watkins, E. B.; Lassègue, B.; Griendling, K. K.; Bowen, J. P., Design, synthesis, and

biological evaluation of inhibitors of the NADPH oxidase, Nox4. *Bioorg Med Chem* **2018,** *26* (5), 989-998.

87. Orloff, D. G., Fixed combination drugs for cardiovascular disease risk reduction: regulatory approach. *Am J Cardiol* **2005,** *96* (9a), 28K-33K; discussion 34K-35K.

88. Schrödinger, L. *Small-Molecule Drug Discovery Suite 2014-1.*, New York, 2014.

89. Biffinger, J. C.; Kim, H. W.; DiMagno, S. G., The polar hydrophobicity of fluorinated compounds. *Chembiochem* **2004,** *5* (5), 622-7.

90. Pushpakom, S.; Iorio, F.; Eyers, P. A.; Escott, K. J.; Hopper, S.; Wells, A.; Doig, A.; Guilliams, T.; Latimer, J.; McNamee, C.; Norris, A.; Sanseau, P.; Cavalla, D.; Pirmohamed, M., Drug repurposing: progress, challenges and recommendations. *Nat Rev Drug Discov* **2019,** *18* (1), 41-58.

91. Lupkin S, D. H., When Medicine Makes Patients Sicker. *Kaiser Health News.* 2014.

92. Cha, Y.; Erez, T.; Reynolds, I. J.; Kumar, D.; Ross, J.; Koytiger, G.; Kusko, R.; Zeskind, B.; Risso, S.; Kagan, E.; Papapetropoulos, S.; Grossman, I.; Laifenfeld, D., Drug repurposing from the perspective of pharmaceutical companies. *Br J Pharmacol* **2018,** *175* (2), 168-180.

93. Xu, M.; Lee, E. M.; Wen, Z.; Cheng, Y.; Huang, W. K.; Qian, X.; Tcw, J.; Kouznetsova, J.; Ogden, S. C.; Hammack, C.; Jacob, F.; Nguyen, H. N.; Itkin, M.; Hanna, C.; Shinn, P.; Allen, C.; Michael, S. G.; Simeonov, A.; Huang, W.; Christian, K. M.; Goate, A.; Brennand, K. J.; Huang, R.; Xia, M.; Ming, G. L.; Zheng, W.; Song, H.; Tang, H., Identification of small-molecule inhibitors of Zika virus infection and induced neural cell death via a drug repurposing screen. *Nat Med* **2016,** *22* (10), 1101-1107.

94. Nosengo, N., Can you teach old drugs new tricks? *Nature* **2016,** *534* (7607), 314-6.

95. Stone, T. W.; Perkins, M. N., Quinolinic acid: a potent endogenous excitant at amino acid receptors in CNS. *Eur J Pharmacol* **1981,** *72* (4), 411-2.

96. Nakanishi, S., Molecular diversity of glutamate receptors and implications for brain function. *Science* **1992,** *258* (5082), 597-603.

97. Guillemin, G. J.; Meininger, V.; Brew, B. J., Implications for the Kynurenine Pathway and Quinolinic Acid in Amyotrophic Lateral Sclerosis. *Neurodegenerative Diseases* **2005,** *2* (3-4), 166-176.

98. Amin, S. A.; Adhikari, N.; Jha, T.; Gayen, S., First molecular modeling report on novel arylpyrimidine kynurenine monooxygenase inhibitors through multi-QSAR analysis against Huntington's disease: A proposal to chemists! *Bioorg Med Chem Lett* **2016,** *26* (23), 5712-5718.

99. Krausz, F.; Breliere, J. C.; Vaillant, J.; Brunaud, M.; Navarro, J., [A new nonsteroidal anti-inflammatory agent: bucloxic acid (804 CB)]. *Arzneimittelforschung* **1974,** *24* (9a suppl), 1364-7.

100. Ammitzbøll, F., A long-term assessment of the efficacy and safety of multiple oral doses of fenbufen in patients with rheumatoid arthritis. *Scand J Rheumatol Suppl* **1979,** (23), 11-3.

101. Srinivas, C.; Haricharan Raju, C. M.; Acharyulu, P. V. R., A Simple Procedure for the Isolation of γ-Oxobenzenebutanoic Acid Derivatives: Application to the Synthesis of Fenbufen. *Organic Process Research & Development* **2004,** *8* (2), 291-292.

102. Newby, Z. E. R.; O'Connell, J. D., 3rd; Gruswitz, F.; Hays, F. A.; Harries, W. E. C.; Harwood, I. M.; Ho, J. D.; Lee, J. K.; Savage, D. F.; Miercke, L. J. W.; Stroud, R. M., A general protocol for the crystallization of membrane proteins for X-ray structural investigation. *Nat Protoc* **2009,** *4* (5), 619-637.

103. Brogden, R. N.; Heel, R. C.; Speight, T. M.; Avery, G. S., Fenbufen: a review of its pharmacological properties and therapeutic use in rheumatic diseases and acute pain. *Drugs* **1981,** *21* (1), 1-22.

104. Information, N. C. f. B. PubChem Compound Summary for CID 3335, Fenbufen. (accessed December 7).